

PEOPLE'S DEMOCRATIC REPUBLIC OF ALGERIA
MINISTRY OF HIGHER EDUCATION AND SCIENTIFIC RESEARCH
IBN KHALDOUN UNIVERSITY OF TIARET



FACULTY OF APPLIED SCIENCES

Department of Civil Engineering

Study submitted in partial fulfillment of the requirements for

The degree of Master

Specialty: Civil Engineering

Option: Structures

Presented by

BOUREZG Maroua Ikram Souria

Study Topic

**Theoretical approach for bending analysis of thick
exponentially graded plates**

Defended publicly on ...23 /06/2022 before the jury composed of

Mrs. OUAZIR Khatima	President
Mr. DRAICHE Kada	Supervisor
Mr. FELLOUH Mohamed	Co-supervisor
Mr. TLIDJI Youcef	Examiner
Mr. BENFERHAT Rabia	Examiner
Mrs. ZOUATNIA Nafissa	Examiner

Graduating class: 2023/2024

Acknowledgements

We all have mental barriers that prevent us from achieving our goals and one of my goals was the graduation. my graduation day is proud day for me and for my family That's why, above all, I thank Allah for giving me health, determination, will, ability and patience to complete my university career and make my parents proud of me.

A huge Thank to my supervisor I express my deep thanks to Mr. DRAICHE Kada for his support, guidance, presence at every step of this work and for not rejecting my desire to do this work in English. It was a great honor for me to be his student and very pleased to oversee my graduation project, his knowledgeable advice, his great availability, as well as his profound humanity and his encouragement which have been very useful to me in carrying out this work. I could not do this alone without him thank him for standing by me.

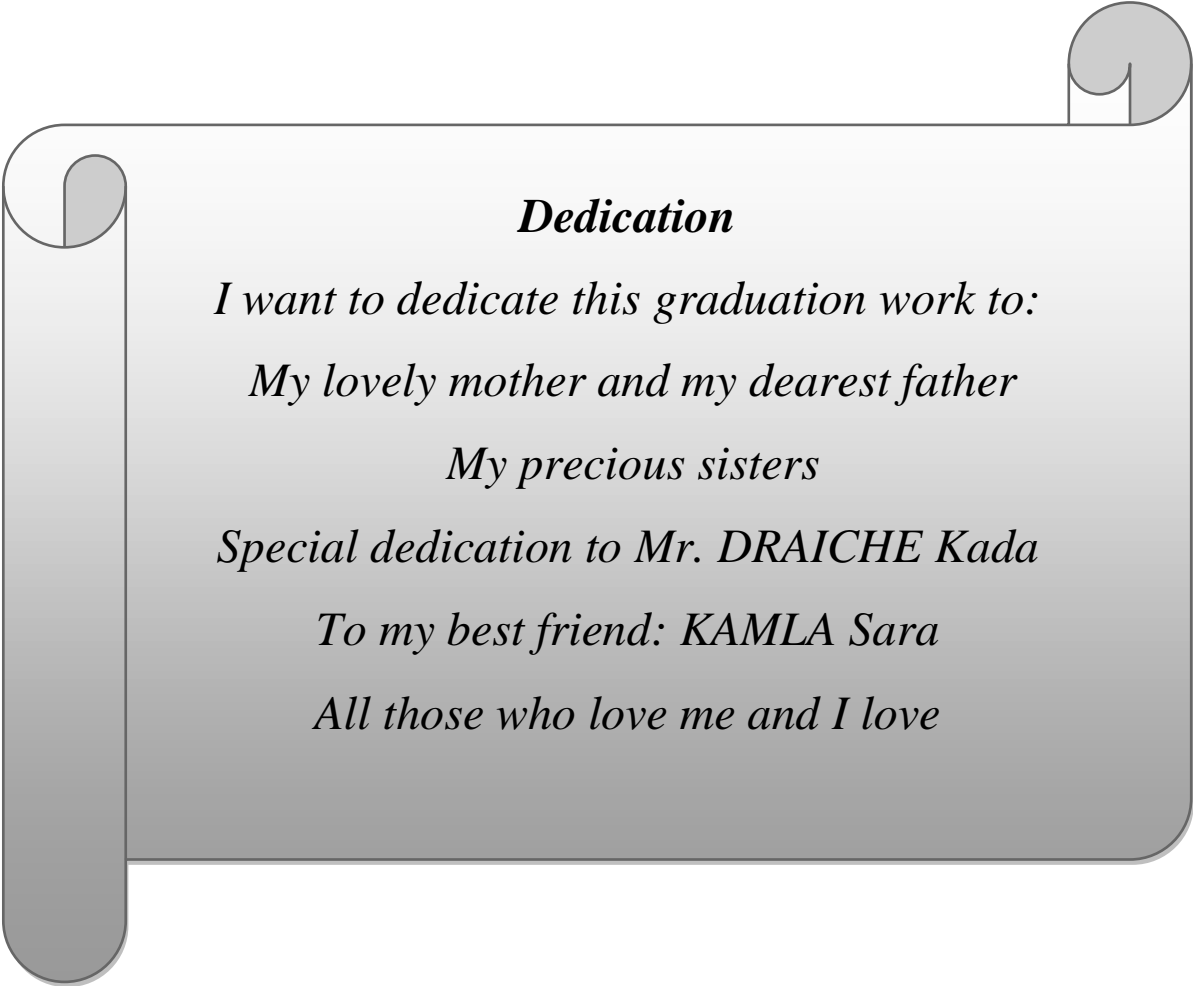
I want to thank the jury members very much:

- Mrs. OUAZIR Khatima for having agreed to examine this work and for having honored me to chair the jury*
- Mrs. HADJI Nafissa, who also agreed to examine this study, I want to thank her.*
- Mr. TLIDJI Youcef, who has given me the honor of examining this work and I am deeply grateful for it.*
- Mr. BENFARHAT Rabia who accepted to be an examiner, I sincerely thank him.*
- I warmly thank madam HADJI who honored me in the presence of my graduation especially for her extreme kindness*
- I express great gratitude to Mr. MIMOUNI Mohamed and Mr. FELLOUH Mohamed I sincerely thank them for all the help they have given me.*

A special Thank to myself for being stronger than ever against every single hurdle I would like to express my sincere and heartfelt gratitude to my parents, thank you my beautiful mom for your existing from when I was a child until today, you have given me the courage in my hardest time, thank you for your faith in how far I can go, thank you my father my soldier for your sacrifices you have great role in my life.

I would like to thank the beautiful babies in the universe Mahira and Khaled, dear sisters I would like to say thank you for the encouragement and support you have given me over and over again specially Rachida and Fahima. I want to thank my dear friend KAMLA Sarah for her continued support all through those years of study.

- *“Education is our passport to the future, for tomorrow belongs to the people who prepare for it today”. — Malcolm X*



Dedication

I want to dedicate this graduation work to:

My lovely mother and my dearest father

My precious sisters

Special dedication to Mr. DRAICHE Kada

To my best friend: KAMLA Sara

All those who love me and I love

Figures List

Chapter I

Figure I.1: Forms of FGM presence in nature [22]. - 5 -

Figure I.2: Representation of a typical functionally graded material [28]. - 8 -

Figure I.3: A functionally graded plate in the reality [23] - 8 -

Figure I.4: The mixed powder centrifugal method [27]. - 10 -

Figure I.5: Schematic of the process for producing graded materials by slip casting [30]. - 10 -

Figure I. 6: Principle of strip casting [27]. - 11 -

Figure I.7: Principle of Plasma projection [31]. - 11 -

Figure I. 8: A schematic view of the chemical vapor deposition process [32]. - 12 -

Figure I.9: Beam Assisted Deposition (IBAD) Process [32]. - 13 -

Figure I.10: Concept of thermal spraying [32]. - 13 -

Figure I.11: Classification of FGM structures [24]. - 14 -

Figure I.12: Classification of FGM based on type of FGM gradients [33]. - 15 -

Figure I.13: The role of the interface on the toughness of composites [4]. - 16 -

Figure I.14: Forms of FGM presence in nature [22]. - 16 -

Figure I.15: Geometry of a plate made of materials with gradient properties [3]. - 18 -

Figure I.16: Volume fraction of the constituents $V(z)$ along the thickness of a P-FGM plate for various values of the power-law exponent p - 19 -

Figure I.17: Volume fraction of the constituents $V(z)$ along the thickness of a S-FGM plate for various values of the power-law exponent p - 20 -

Figure I.18: Volume fraction of the constituents $V(z)$ along the thickness of an E-FGM plate for various values of the power-law exponent p - 21 -

Figure I.19: Various fields of Application of FGMs [21]. - 21 -

Chapitre II

Figure II.1: Model of an FGM plate. - 24 -

Figure II.2: Application Area [24]. - 26 -

Chapitre III

Figure III. 1: Geometry of an exponentially graded plate model - 43 -

Chapitre IV

- Figure IV.1:** Distribution of non-dimensional axial displacement (\bar{u}) across the thickness of EG square and rectangular plates ($a/h = 4, p = 0.5$) - **61** -
- Figure IV.2:** Distribution of non-dimensional axial displacement (\bar{v}) across the thickness of EG square and rectangular plates ($a/h = 4, p = 0.5$) - **61** -
- Figure IV.3:** Distribution of non-dimensional transverse displacement (\bar{w}) across the thickness of EG square and rectangular plates ($a/h = 4, p = 0.5$) - **62** -
- Figure IV.4:** Distribution of non-dimensional axial stress ($\bar{\sigma}_{xx}$) across the thickness of EG square and rectangular plates ($a/h = 4, p = 0.5$) - **62** -
- Figure IV.5:** Distribution of non-dimensional in-plane shear stress ($\bar{\tau}_{xy}$) across the thickness of EG square and rectangular plates ($a/h = 4, p = 0.5$) - **63** -
- Figure IV.6:** Distribution of non-dimensional transverse shear stress ($\bar{\tau}_{xz}$), through the thickness of EG square and rectangular plates ($a/h = 4, p = 0.5$) - **63** -
- Figure IV.7:** Distribution of non-dimensional transverse shear stress ($\bar{\tau}_{yz}$), through the thickness of EG square and rectangular plates ($a/h = 4, p = 0.5$) - **64** -

Tables List

Chapter I

Table I.2: Comparison of the mechanical properties between ceramics and metals..... - 18 -

Chapter II

Table II.1: Different shear functions of isotropic plate theories and FGM as well as a comparison between the different models. - 33 -

Chapter IV

Table IV.1: Non-dimensional transverse displacement $w(a/2, b/2, 0)$ for various power-law exponent of EG square and rectangular plates, $a/h = 2$ - 54 -

Table IV.2: Non-dimensional transverse displacement $w(a/2, b/2, 0)$ for various power-law exponent of EG square and rectangular plates, $a/h = 4$ - 55 -

Table IV.3: Non-dimensional transverse displacement $w(a/2, b/2, 0)$ for various power-law exponent of EG square and rectangular plates, $a/h = 10$ - 56 -

Table IV.4: Non-dimensional in-plane normal stresses $\bar{\sigma}_{xx}(a/2, b/2, h/2)$ for various power-law exponent of EG square and rectangular plates, $a/h = 10$ - 57 -

Table IV.5: Non-dimensional in-plane normal stresses $\bar{\sigma}_{yy}(a/2, b/2, h/2)$ for various power-law exponent of EG square and rectangular plates, $a/h = 4$ - 58 -

Table IV.6: Non-dimensional in-plane normal stresses $\bar{\sigma}_{yy}(a/2, b/2, h/2)$ for various power-law exponent of EG square and rectangular plates, $a/h = 10$ - 59 -

Table IV.7: Non-dimensional shear stresses $\bar{\tau}_{xz}(0, b/2, 0)$ for various power-law exponent of EG square and rectangular plates, $a/h = 10$ - 60 -

Abbreviation and Notation List

FGM: Functionally graded Materials

C.V.D, P.V.D: are the chemical and physical vapor depositions, respectively

IBAD: Ion Beam-assisted Deposition

PED: Pulsed Electro-Deposition technique

P-FGM: The power-law distribution

E-FGM: The exponential-law distribution

S-FGM: The sigmoid-law distribution

p : Power-law exponent

z : Present coordinated according to thickness and it is the varying direction

$V(z)$: Volume fraction

E : Young's modulus

$E(z)$: Young's modulus according to z

E_c : Young's modulus of ceramic

E_m : Young's modulus of metal

h : The plate thickness

a : The length of the plate.

b : The width o the plate

x, y, z : Cartesian coordinate system

2D, 3D: Two-dimensional and three-dimensional, respectively

u, v, w : The displacement according to x, y and z directions respectively.

u_0, v_0, w_0 : The displacements components along the average plane of the plate

∂ : Partial derivative

δ : The variational operator

ϕ_x, ϕ_y : The rotations of the normal to the cross section with respect to the y and x axes, respectively

$f(z)$: The shape function

$g(z)$: Derivative of the shear function

w_b, w_s : The bending and shear components of the transverse displacement

ν : Poisson's ratio

$\theta(x, y)$: The rotations value of the normal to the mid-plate according to the x and y axes.

k_1, k_2 : coefficients depend on the geometry of the considered plate

$\int \theta(x, y)dx, \int \theta(x, y)dy$: The indeterminate integral variables

$\sigma_x, \sigma_y, \sigma_z$: Normal stresses

$\tau_{xy}, \tau_{xz}, \tau_{yz}$: Shear stresses

$\varepsilon_x, \varepsilon_y, \varepsilon_z$: Strains according to x, y and z axis

$\gamma_{xy}, \gamma_{xz}, \gamma_{yz}$: Distortion deformations

$\delta u, \delta v, \delta w$: Virtual displacement field

δU : Variation of deformation energy

δV : External virtual work variation

N_x, N_y, N_{xy} : Normal forces

M_x^b, M_y^b, M_{xy}^b : Bending moments

M_x^s, M_y^s, M_{xy}^s : Moment due to transverse shear stresses

S_{xz}, S_{yz} : Additional moment due to transverse shear stresses

$A_{ij}, B_{ij}, D_{ij}, E_{ij}, F_{ij}, H_{ij}, A_{ij}^s$: The plate stiffness coefficients

$q(x, y)$: The transverse load which is spreading on the top surface of the plate

q_0 : The maximum intensity of distributed load at the plate centre

Q_{ij} : The elastic constants

$U_{mn}, V_{mn}, W_{mn}, \Theta_{mn}$: The unknown coefficients

$[K_{ij}]$: Stiffness matrix

ملخص

في هذه الدراسة، تم تقديم نظرية جديدة عالية المستوى منقحة لسلالة القص المكافئ "PSDPT" لتحليل انحناء الصفائح السميكة المتدرجة أسياً "EG". الميزة الرئيسية لهذا النموذج هي أنه يعتمد على مجال إزاحة بسيط ومحسّن ثنائي الأبعاد مع أربعة متغيرات غير معروفة فقط، وهو أقل حتى من نظريات تشوه القص الأخرى التي تتضمن خمسة متغيرات مجهولة أو أكثر. تعتبر النظرية الحالية أن دالة الشكل المكافئ غير الخطية تلبّي تمامًا ظروف إجهاد القص الصفري على الأسطح الخارجية للصفائح دون استخدام عامل تصحيح القص. من المفترض أن تختلف الخواص الميكانيكية للصفائح المتدرجة وظيفياً بشكل مستمر في اتجاه السُمك وفقاً للقانون الأسّي "E-FGM" تم استخلاص المعادلات الحاكمة وكذلك شروط حدود الصفيحة من خلال تطبيق مبدأ العمل الافتراضي. للتحقق من صحة هذه النظرية، يتم التأكد من النتائج التحليلية المحسوبة للصفائح السميكة EG المربعة والمستطيلة المدعومة ببساطة بتقنية Navier-Type مع تلك التي تم الحصول عليها من خلال نماذج تشوه القص الأخرى وحلول المرونة ثلاثية الأبعاد التي تم أخذها في الاعتبار. تمت مناقشة تأثير العوامل المهمة على نتائج الإجهاد الميكانيكي.

الكلمات المفتاحية: صفيحة التدرج الوظيفي "EG"؛ PSDPT؛ تحليل الانحناء؛ مجال الإزاحة ثنائي الأبعاد المحسّن.

Abstract

In this study, new refined higher-order parabolic shear deformation theory "PSDPT" for the bending analysis of thick exponentially graded "EG" plates is presented. The main advantage of this model is that it relies on a simple and optimized 2D displacement field with only four unknown variables, This is even less than other shear strain theories that involve five or more unknowns. The present theory considers a function of nonlinear parabolic form to satisfy exactly the zero shear stress conditions on the outer surfaces of the plates without using the shear correction factor. The mechanical properties of functional gradient plates are assumed to vary continuously in the thickness direction along an exponential law distribution "E-FGM". The governing equations as well as the boundary conditions of the plate are derived by implementing the principle of virtual work. To verify the accuracy of this theory, the analytical results calculated for simply supported thick square and rectangular EG plates by the Navier-Type technique are verified with those obtained by other shear strain models and 3D elasticity solutions considered in the literature. Influence of important parameters on the results of mechanical stresses are discussed.

Keywords: Functionally graded "EG" plate; PSDPT; bending analysis; optimized 2D displacement field.

Résumé

Dans cette étude, une nouvelle théorie raffinée d'ordre élevé de déformation en cisaillement parabolique "PSDPT" est présentée pour l'analyse de la flexion de plaques épaisses à gradation exponentielle "EG". Le principal avantage de ce modèle est qu'il s'appuie sur un champ de déplacement 2D simple et optimisé avec seulement quatre variables inconnues, ce qui est encore moins que les autres théories de déformation en cisaillement qui impliquent cinq inconnues ou plus. La présente théorie considère une fonction de forme parabolique non linéaire pour satisfaire exactement les conditions de contrainte de cisaillement nulle sur les surfaces extérieures des plaques sans utiliser le facteur de correction de cisaillement. Les propriétés mécaniques des plaques à gradient fonctionnel sont supposées varier de manière continue dans le sens de l'épaisseur le long d'une loi exponentielle "E-FGM". Les équations gouvernantes ainsi que les conditions aux limites de la plaque sont dérivées en mettant en œuvre le principe du travail virtuel. Pour vérifier l'exactitude de cette théorie, les résultats analytiques calculés pour les plaques épaisses EG carrées et rectangulaires simplement appuyées par la technique Navier-Type sont vérifiés avec ceux obtenus par d'autres modèles de déformation de cisaillement et solutions d'élasticité 3D considérées dans la littérature. L'influence de paramètres importants sur les résultats des contraintes mécaniques sont discutées.

Mots clés : Plaque à gradient fonctionnel "EG" ; PSDPT ; analyse de la flexion ; champ de déplacement 2D optimisé.

Table of contents

Acknowledgment.....	i
Dedication	ii
Figures List	iii
Table List	iv
Abbreviation and Notation List.....	v
Abstract.....	vi
General Introduction	1

Chapter I

General information on FGM

I.1. Introduction.....	5
I.2. Literature review	6
I.3. History of the development of FGM materials	7
I.4. Manufacturing technique for FGM	8
I.4.1. Bulk FGM manufacturing technique (Conventional techniques)	9
I.4.1.1. Powder metallurgy.....	9
I.4.1.2. Dry compaction of powders	9
I.4.1.3. Centrifugal casting.....	9
I.4.1.4. Slip casting	10
I.4.1.5. Tape casting (strip casting)	11
I.4.1.6. Plasma projection	11
I.4.2. Thin FGM manufacturing techniques (advanced technique).....	12
I.4.2.1. Vapor deposition	12
I.4.2.2. Ion beam-assisted deposition	12
I.4.2.3. Electro- deposition.....	13
I.5. Classification of FGMs.....	13
I.5.1. Classification based on FGM structure	13
I.5.2. Classification based on FGM gradient type.....	14
I.6. Comparison of FGM Materials and Traditional Materials	15
I.7. Governing laws of the material properties variation of FGM plate	18
I.7.1. Material properties of P-FGM plate	19

I.7.2. Material properties of S-FGM plate	20
I.7.3. Material properties of E-FGM plate	20
I.8. Application Area	21
I.8.1. Thermal barrier	22
I.8.2. Defense	22
I.9. Advantages and disadvantages of functionally graded materials	22
I.9.1. Advantages of Functionally graded materials	22
I.9.2. Disadvantages of FGMs	22
I.10. Conclusion	22

Chapter II

The different theories of FGM plates

II.1. Introduction	24
II.2. Definition of the plates	24
II.3. Different types of plates	25
II.3.1. Isotropic plates	25
II.3.2. Orthotropic plates	25
II.3.3. Anisotropic plates	25
II.4. Application Area	25
II.5. Different types of theories	26
II.5.1. Bi-dimensional theories	27
II.5.1.1. Classical plate theory (CPT)	27
II.5.1.2. First shear deformation theory (FSDT)	28
II.5.1.3. High- order shear deformation theory (HSDT)	30
II.5.1.4. Refined plate theory (RPT)	35
II.5.1.5. Higher-order shear and normal deformation theory (qausi-3D)	35
II.5.2. Three-dimensional theory (3D)	36
II.6. Layered approach	37
II.6.1. Zig-zag approach	37
II.6.2. Discret layer models	39
II.7. Conclusion	40

Chapter III

Theoretical approach for bending analysis of thick exponentially graded plates

III.1.Introduction	42
III.2.Mathematical formulation of present approach.....	42
III.2.1.Exponentially graded plate model	42
III.2.2. Theoretical formulation assumptions.....	43
III.2.3.kinematic and constitutive relations	43
III.3.Governing differential equations	46
III.4.Analytical solution for EG plates	49
III.5.Conclusion.....	50

Chapter IV

Numerical results and discussion

IV. 1. Introduction	52
IV.2. Numerical results and discussion	52
IV.2.1. Validation study.....	53
IV.2.2.Parametric study	60
IV.3.Conclusion	64
General conclusion	65
Bibliographic references	66



General Introduction

General introduction

For the need to adapt and meet the human needs that are increasing day by day, humanity is witnessing the tremendous progress of science in various industrial fields by improving various researches including materials science.

Materials are a promising research component because of their necessary study that gives their applications a presence in various fields. The development of these materials creates a continuous presence of revolution in the industrialized world because of its importance in achieving desired results on the technological side.

The fact that conventional metal materials are beginning to show their limits in the face of parts and machinery design, because their resistance to heat stress is very limited; Composite materials have been developed to find solutions to these limits, and these materials are made of more than one material with a fairly high strength/weight ratio; this latter has been successfully used in the aviation industry and other technological applications.

The composite material consists of two or more substances of different nature, its combination results excellent performance that exceeds the performance of separately taken components; which can provide the best properties such as hardening, fatigue strength, corrosion resistance. Although these composite materials present an interface problem and discontinuity of properties of the layers, the latter causes high levels of stress concentration, matrix cracking and delamination which are caused by sudden passage through the material component especially in a high temperature environment. Moreover, this issue makes us face long term concerns that can be represented by the large plastic deformation on the interface leading to the propagation of cracks [1].

For that reason, functional gradient materials have emerged. These materials are considered as alternative choice used in the reduction of the aforementioned problems by the gradual variation in the volume fraction of the constituents, inducing changes and eliminating discontinuities at interfaces, while the properties of the materials are preserved [2] whose mechanical and thermal properties vary continuously across the thickness of the material [3]. FGMs were initially designed as thermal barrier material is for aerospace structural applications and fusion reactors. They are now developed for general use as structural components in extremely high-temperature environments. FGMs are now recognized as important composite materials throughout the world. Utilization of FGMs appears to be one

of the most efficient and effective materials in achieving sustainable development in Industries [4].

Currently, many researchers have consecrated their time in structural applications to achieve the additional function such as hardness machine ability to the heat resistance, wear by combining two components, like the ceramic and the metal [2].

The FGM plates that are the subject of this study are made from a mixture of metal and ceramic. These latter are widely used in aerospace, automotive, civil and mechanical engineering structures and their material properties can be adapted to different applications and working environments [3].

The field equations for a functionally graded plate is derived by Cheng and Batra [5] using the first-order shear deformation theory or the third-order shear deformation theory which are simplified for a simply supported polygonal plate. Javaheri et al. [6] used a higher-order shear deformation plate theory and the Navier type solution to investigate the thermal buckling of simply supported FG plates under different types of thermal loads. Kashtalyan [7] proposed a 3D elasticity solution for a simply supported FG plate subjected to transversely distributed loads. Carrera et al. [8] have applied a unified formulation and the principle of virtual displacements to derive finite element solutions for the static analysis of FG plates subjected to transverse mechanical loads. Ferreira et al. [9] applied a Meshless method to static analysis of simply supported functionally graded plate, employing a third-order shear deformation theory. Elishakoff et al. [10] formulated a three-dimensional elasticity solution utilizing the Ritz method to evaluate the static response of a clamped rectangular FG plate, with determined material properties through a power-law distribution. Zenkour [11] presented the static response of FG plates using the generalized shear deformation theory developed by Mantari and Guedes Soares [1]. Chi and Chung [12] studied the mechanical behavior of FGM plates under transverse loads, examining three property evaluation methods: power-law, sigmoid, or exponential functions. Zenkour [13] investigated the static problem of transverse loads on EGM rectangular plates, employing both 2D trigonometric shear deformation plate theory (TSDPT) and a 3D elasticity solution. An analytical solution for the static governing equations of exponentially graded plates is achieved using a new trigonometric higher-order shear deformation plate theory (HSDPT) developed by Mantari et al. [14] to facilitate comparison, the widely used HSDPT, initially formulated by Levy [15] and refined by Stein [16], extensively employed by Touratier [17], and recently adapted to FGM and exponentially graded material (EGM) by Zenkour [13], is reproduced and expanded to cover EGM. This

replication is necessitated by Zenkour's previous work, without considering stretching effects, and Zenkour's separate investigation focusing solely on EGM, this time considering the stretching effect. These theories effectively distribute transverse shear stresses throughout the plate thickness and maintain tangential stress-free boundary conditions on the plate's boundary surface, avoiding the need for a shear correction factor. Thom et al. [18] used an accurate computational approach based on finite element method and a new third-order shear deformation plate theory for the bending and buckling behaviors of 2D-FGM plates under statically mechanical loading. Bennai et al. [19] used a four variable plate theory to study the dynamic and wave propagation of FGM plates with porosities, in which a new form of porosity distribution depending on the plate thickness was employed. Recently, Zaiton et al. [20] used an efficient mathematical model based on high-order sinusoidal shear deformation theory for vibration behavior of a functionally graded sandwich plate resting on a visco-elastic foundation, and subjected to a hygro-thermal environment loading.

The first main objective of our study is to determine the mechanical behavior of the FGM plate by a new analytical model based on higher-order plate theory to determine the equilibrium equations of an FGM plate and to compare the results obtained with the results of other models proposed in the literature. The mechanical properties of the plates are assumed to vary exponentially in the thickness direction. Unlike other theories, the number of unknown functions for the proposed theory is only four, while other theories have five or more. This refined theory is variationally consistent, does not require a shear correction factor and allows a parabolic distribution of shear stress through thickness while fulfilling the condition of zero shear stress on the upper and lower free surfaces. So the use of this materials is not possible unless through theories that enable us to study and analyze their response. In our study we will focus on the higher-order shear deformation plate theory (HSDPT) and higher-order shear and normal deformation theory.

Problematic

After a literature check of the latest published papers, the majority of research focuses on the study of the bending behavior of FGM plates by using the power law P-FGM. There has been little investigation on bending of the E-FGM plates using the displacement field containing integrals with four-variable.

Objective

This work makes a contribution to study the static response of FG thick simply supported plates by using a new parabolic shear deformation plate theory (PSDPT).

Organization of chapters

This work is structured into four chapters as follows:

After a general introduction on the topic of functionally graded materials (also known as property gradient materials or functionally modified materials graduates) as well as the theme developed in the framework of this topic.

Chapter I: General information on functionally graded materials

Therefore the first chapter, we try to present a bibliographical study on the new class of composites designated by functional gradient materials, discussing the scientific research for the development of the latter as well as the different manufacturing processes and their interests through sectors of modern industry.

Chapter II: The different theories of FGM plates

In this chapter we present a general review of the different plate theories developed in the literature to improve the evolution of the variation of the displacement field through the thickness and for the modeling and analysis of plates FGM. In principle the study is based on equivalent single-layer models (ELS; Equivalent Single Layer), such as CPT, FSDPT, HSDPT, RSDPT and Quasi-3D plate theories.

Chapter III: Bending analysis of EG plates

The new displacement field of the present parabolic shear deformation plate theory takes into account the transverse shear effect of EG plates, whose material properties vary across the thickness direction according to an exponential function (E-FGM). Through the development of theoretical formulations based on the principle of virtual work and Navier solution method, we can build an analytical bending model for simply supported EG plates.

Chapter IV: results and discussions

This chapter is devoted to the results obtained by the present analytical development. Results are furnished for thick plates across various values of the power-law exponent, dictating the material variation profile across the plate thickness. The accuracy of the developed code is validated through comparison with 3D elasticity solutions and other established shear deformation theories.

Finally, our work ends with a general conclusion.

 *Chapter I*

General information on FGM

Chapter I

General information on FGM

I.1. Introduction

Functionally graded materials (FGMs) comprise a continuous variant of material characteristics which arise from the in-homogeneous microstructure [21]. Most of FGMs are customarily found in nature (Figure I-1) such as the varying spongy trabecular structures of bone or local tissue variation in seashells for example pearl oyster, *Cypracassis rufa*, a *Peristernia incarnate*; plus the plants like Norway spruce and bamboo [22].

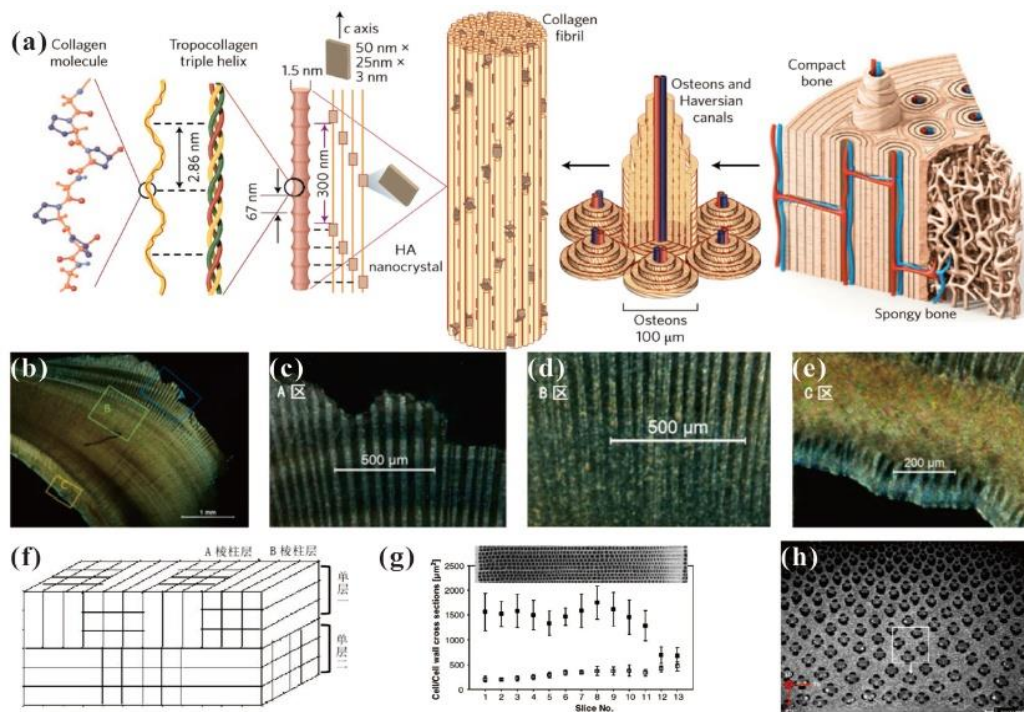


Figure I.1: Forms of FGM presence in nature [22].

Thanks to the superior graded materials properties (specific high strength and high stiffness) FGMs have been considered to have a great interest in many lines with immense applications, including aerospace, biomaterials and engineering among other fields in the past decades. The (FGMs) owned microstructure, chemical composition or atomic order that is influenced by the position, which can appear in the continuous variation of material properties such as mechanical, electrical and thermal properties [21].

FGMs have been used extensively in various applications of engineering branches to serve the needs of the structure and in different fields of industry to make optimum use of their

potential characteristics. The two major ones are the aerospace and biomedical. In the aerospace field they have numerous benefits that make them appropriate in efficient applications. It involves a possible reduction of plane transverse stresses through-the thickness, improved thermal properties, high toughness, etc [3].

In addition to Composite materials are classified as developed materials, which involve one or more materials integrated in solid states with specific physical and chemical properties [21]. Composite materials are man-made materials and its components combined in order to create a useful material of optimum use with enhanced and desired properties (high strength, high stiffness, excellent corrosion resistance, greater fatigue life, low weight) [23]. This new notion makes the beginning of a revolution in the fields of materials science and mechanics [4].

I.2. Literature review

Around 1984-1985 , two Japanese researchers, one in the field of aeronautics and the other one in the field of materials science dream of designing a spacecraft in the coating could hold out a very glaring thermal environment. There was no metallic material or composite material able to meeting both the environmental exigencies as described while sustaining excellent mechanical properties. They then were swapping the idea of the FGM concept, that is to say a material with a continuous gradation in the direction of thickness passing from a totally metallic face to a totally ceramic face. In 1987, the national FGM research and development program was instituted in Japan [4]. Many researchers from public institutions and industry have collaborated to originate a new type of material, fundamentally to help build the outer shell of a hypersonic space shuttle. The main issue to be solved being the massive heat flow beating the plurality of surfaces which are subjected to friction by air. While the shuttle's re-entry period into the Earth's atmosphere and at the same time, to keep the internal part protected against thermal collision [24].

The idea at that time was about develop a new composite called functional gradient material to taking advantage of the properties of ceramics (high temperature side) and metals (low temperature side) [7] with the production of a smooth transition between pure metal and pure ceramic [4].

Generally, FGMs are comparatively new materials known to withstand such thermo-mechanical behavior (buckling) [25], static thermo elastic behavior but few studies have been devoted to the free vibrations of these materials. Since the year 2000 the researchers began to be interested in their dynamic behavior [4].

I.3. History of the development of FGM materials

In the first place, we should mention that the compositional and structural gradient in material microstructure was proposed idea for composites and polymeric materials in 1972. In 1972 many gradient composites was studied by Bever [23], and he investigated the general material characteristics and reviewed possible uses of graded composites. And in 1972 Shen [23] announced that the polymeric material gradation has the possibility to be caused by the chemical nature of the monomers variation, the molecular combining of the polymers and the supra molecular structure or morphology of the polymers, the effectual characteristics such as chemical, mechanical, biomedical and transition properties and potential uses, including the consideration of both the gasoline tank and damping materials. However, the study of this gradient structure's tailoring, manufacturing and evaluation was lacking at that time [23] It wasn't until 1985 that continuous texture control emerged, This concept of continual microstructure control was seen as a way to introduce new properties and functions to materials such as benefit the cohesive forces and minimize the thermal stress in the ceramic coatings and joints and it being developed for usable rocket engine [26]. In 1984 the concept of "Functionally Graded Materials" was developed in the Sendai National Aerospace Laboratory by Mr. Niino and his colleagues [27]. In 1987, the Japanese government launched an extensive project entitled "Research on basic technology for the development of functionally graduated materials and the study of the relaxation of thermal stresses". The interest of the project is to develop materials with structures used as thermal barrier in aerospace programs [26], three characteristics were considered for the design of a material to withstand surface temperatures of 1800°C and a temperature gradient of 1300°C [27]:

- Thermal resistance and high temperature oxidation resistance of the surface layer of the material
- Low temperature at side material toughness
- Effective relaxation of thermal stress along the material

In the 1990s, not only has the application field of FGM developed for structural materials operating at high temperatures, but it has also expanded to other applications [24] since then, FGMs have found widespread use in various applications beyond aerospace, including biomaterials like biomedical implants such as artificial bones and dental implants. Too many researchers had the same opinion and announced that FGMs in the biomedical field could give the implant a suitable rigidity to resist the physiological loading and that the graded porosity structure could make the mechanical property of the implant stronger to improve the materials response to external loading [21].

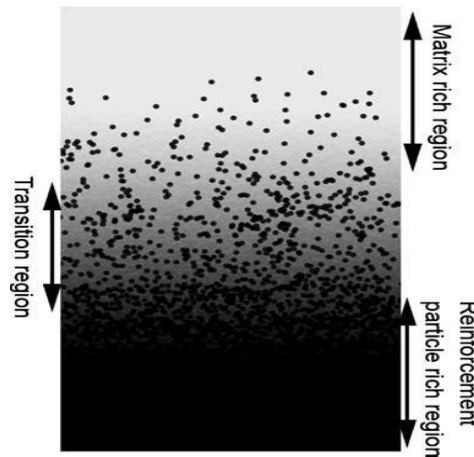


Figure I.2: Representation of a typical functionally graded material [28].

As we can see in Figure (I.2) there is two different regions of two different materials (generally ceramic and metal), and between this regions there is a smooth and continuous change from one region to another of their material properties and that happens by the gradual variation of the volume fraction of constituent materials, thus interface problems can be eliminated and thermal stress concentrations can be mitigated. This is because of the ability of the ceramic constituents of FGMs to withstand high-temperature environments due to their ideal thermal resistance properties, during the metal constituents give stronger mechanical performance and minimize the chances of a fatal fracture [28].

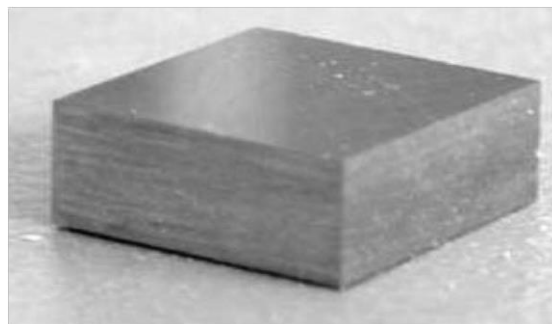


Figure I.3: A functionally graded plate in the reality [23]

I.4. Manufacturing techniques for FGM

The most important part of FGM research is the fabricating process which is based on the conventional treatment processes variation [27].

I.4.1. Bulk FGM processing techniques (Conventional techniques)

Techniques that are able to receiving a grading step contain powder metallurgy and dry compaction processes of powders. Generally, the majority largely used elaboration processes. the most appropriate production method choice depends basically on the combination of the material, the type of the desired batching law and the desired component geometry. This method considered the most commonly employed technique among others because of its wide control on the composition and microstructure and form-forming capacity [27].

I.4.1.1. Powder metallurgy

Powder metallurgy provides more advantages through lower costs, increased obtainability of raw materials, simpler processing equipment, lower energy consumption and shorter processing times. In powder processing, gradient is usually created by the batching of various powders in varying ratios and stacking the powder mixtures in separate layers. Many processes have been presented for powder preparation, for example by chemical reaction, electroplating or grinding. These techniques empower mass production rates of powdered materials and a lot of controllable sizes of the final grain quantity. For powder processing, the first consideration concentrates on the weighing quantities accuracy and dispersion of mixed powders. These elements will affect on the structure properties and should be handled very carefully [25].

I.4.1.2. Dry compaction of powders

This process can be used for the manufacture of parts of complex shapes in this technique the powders are successively poured into a steel mould. After each time of the powder pouring, a weak compression will be carried out. This process is usually followed by iso-static pressure and delamination and the last step is about the execution of the densification [29].

I.4.1.3. Centrifugal casting

Centrifugal casting is considered the most efficient method for processing. This technique has mainly been used to get the cylindrical parts. The basic centrifugal casting machines types are: horizontal types, which rotate around the horizontal axis, and vertical type, which rotate around a vertical axis. In this operation the molten metal is channeled into a rotating mold (usually 700 to 1300 rpm). The Rotation results a centrifugal strength that moves the metal toward the mold wall. The mixed powder centrifugal method shown in Figure (I.4) is another way presented as a limitation solution of the centrifugal casting process in manufacturing FGMs including nano-sized particles [27].

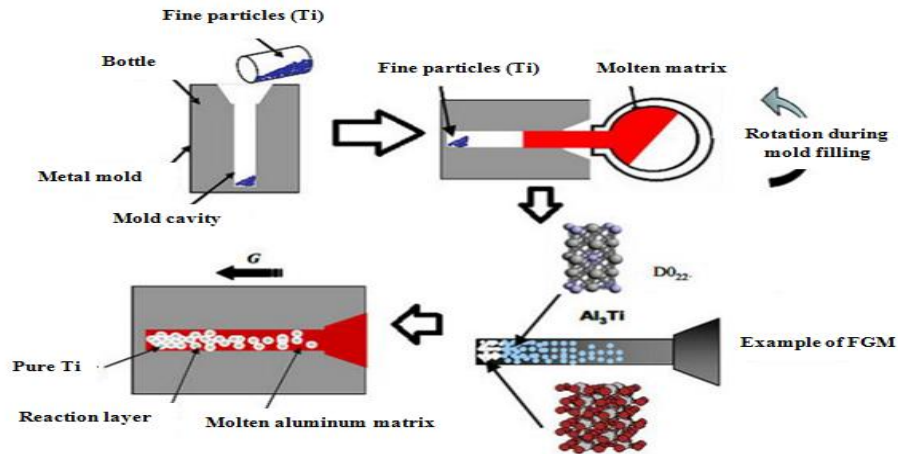


Figure I.4: The mixed powder centrifugal method [27].

I.4.1.4. Slip casting

This technique contains pouring a suspension into a porous mold which will drain the liquid due to capillary forces, it is broken down into two important phases, which are the setting where the shard is shaped and the firming, and in this level the shard is consolidated. Filtration can be considered as a process of eliminating part of the water from the slurry while the pouring, this water emigrates by the shard layer already formed, under the effect of the suction power of the plaster or 'pressure applied to the slip (pressure casting). In the case of the multilayer manufacturing, the deposition of the second layer is carried out after the first shard formation in such a way that the slip does not penetrate into the formed shard. The slip casting is repetitive technique reproduced for the other layers [30].

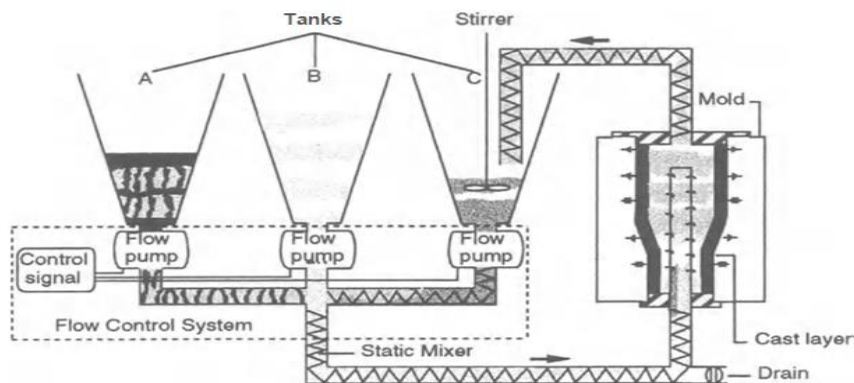


Figure I.5: Schematic of the process for producing graded materials by slip casting [30].

I.4.1.5. Tape Casting (strip casting)

Strip casting is a technique that consists of spreading a slurry of fine powders suspended on a flat surface in thin and regular layers. The spreading is obtained by the relative mobility of a tank. The suspension is thus laminated by its passage between the tank blade and the support as we can see in the Figure (I.6), which gives a uniform thickness for the deposited strip over its entire length. The reservoir knife height relative to the support defines the thickness of the strip. The obtainable products are sheets with controlled thicknesses. After firming of the dough consistency, the sheets are unmolded and then cut [27].

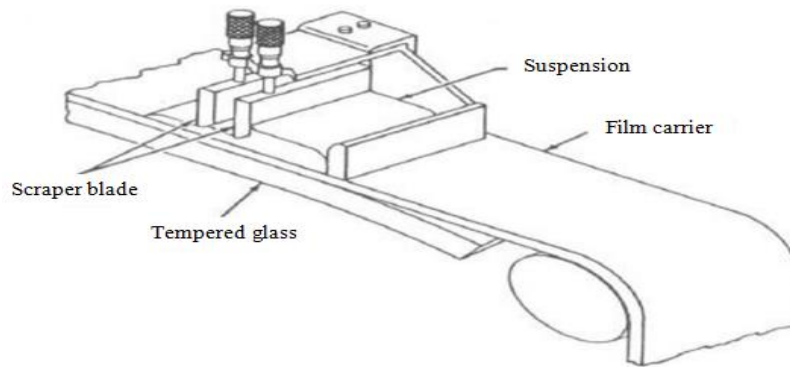


Figure I. 6: Principle of strip casting [27].

I.4.1.6. Plasma projection

In this method we subject a gas to a high temperature which transforms it into an ionized state (plasma). This transformation is accompanied by a huge release of heat. If a ceramic particle is existed in this environment, it melts completely or superficially, and that makes allowed being located on a substrate [31].

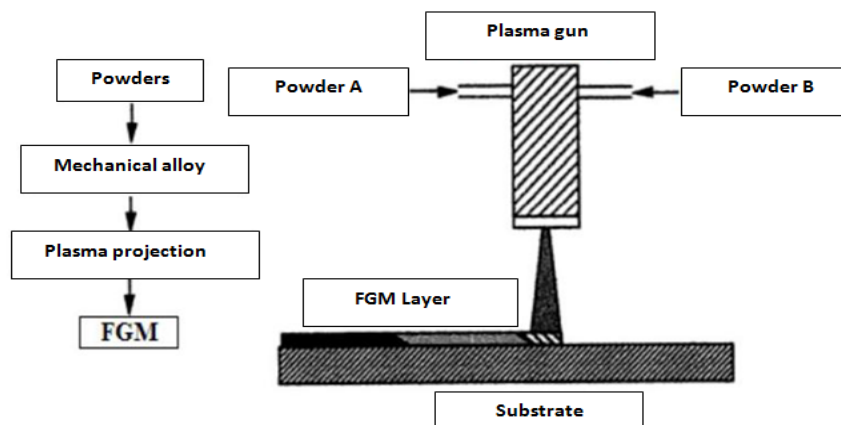


Figure I.7: Principle of Plasma projection [31].

I.4.2. Thin FGM processing techniques (advanced techniques)

I.4.2.1. Vapor deposition

This technique has importance because of its use of iso-static or vacuum hot pressing of desired alloys to produce a composite component. Through this process we are able to get a controlled and thickness deposition, as well as precise layer spacing for laminated grading [32]. Chemical (C.V.D) or physical (P.V.D) vapor depositions are processes for the manufacture of FGM whose atoms of the source material are deposited on the surface of the substrate, The techniques of C.V.D. and P. V. D. can be used for the preparation of FGM on substrates of complicated forms [3].

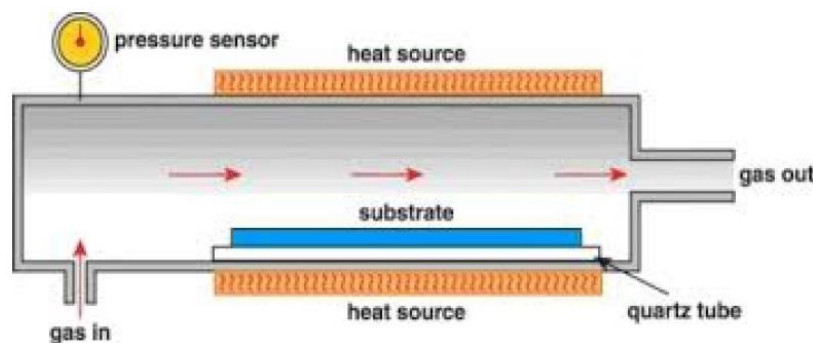


Figure I. 8: A schematic view of the chemical vapor deposition process [32].

I.4.2.2. Ion beam-assisted deposition (IBAD)

Ion Beam Assisted Deposition (IBAD) is considered as most adaptable process of thin film deposition using the blending evaporation technique with simultaneous bombardment in high vacuum environments. The developing films can be modified effectively by bombarding them with high-velocity particles in order to make effective modification in different forms that is essential to the thin coatings activity. We can achieve to these modifications by: orientation variation, increase the developing films at low temperatures, and change the grain size and mechanical properties. This technique can be applicable to deposit coatings of high bond strength, make variation in the concentration of particles for each successive layer through simultaneous bombardment [32].

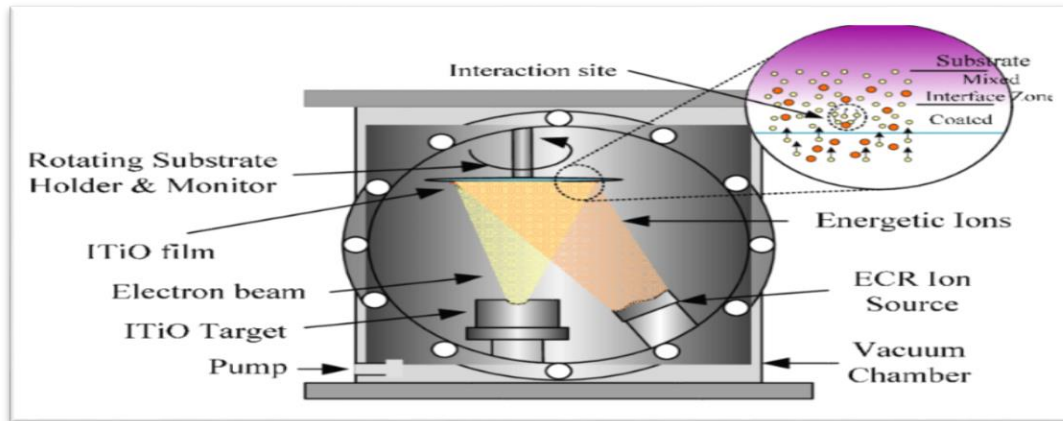


Figure I.9: Beam Assisted Deposition (IBAD) Process [32].

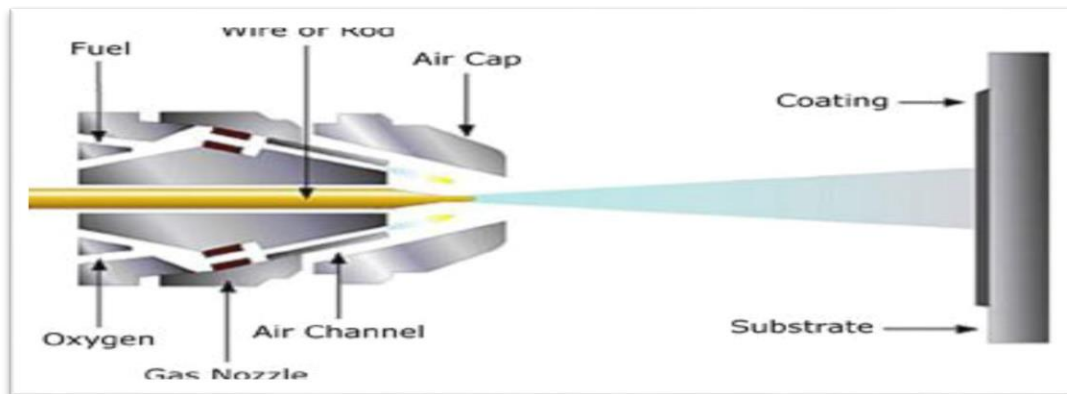


Figure I.10: Concept of thermal spraying [32].

I.4.2.3. Electro-deposition

Recently, electro-deposition has been used to manufacture functionally graded deposits of metal-ceramic composites and bi-metals. That can be happened by the co-deposition of ceramic particles and metallic particles from electrolytes containing the metal ion, with the particle ratio variation or the current density with respect with time. Pulsed Electro-Deposition technique (PED) is a new process utilized to deposit nano-crystalline materials on various metallic substrates [32].

I.5. Classification of FGMs

I.5.1. Classification based on FGM structure

FGM structures contain two general categories (Figure I.11) [25]. The first one is known as continuous gradients, in this category the gradient factor is flowing through the material volume with continuous manner [33], and it is impossible to observe both of the distinct zones and separation cut lines within the material to distinguish the properties of each zone [34].

That is to say, there was neither clear interface between one side and the other nor vestige between them [33]. The second one is called discontinuous gradients, where the gradient factor is changing in discontinuous manner [26], in this category, there is observable interface exists between layers [37] which enables us to distinguish each layer from the next layer (layered or separated FGM) [33].

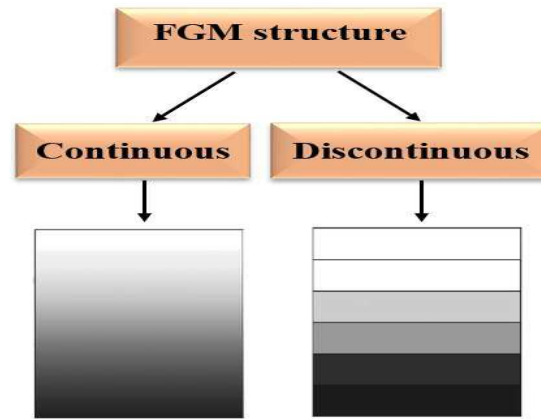


Figure I.11: Classification of FGM structures [24].

I.5.2. Classification based on FGM gradient type

The FGMs are typically divided into three distinct groups as shown in (Figure I.12):

The first group is based on the chemical composition, according to the spatial position in the material; the chemical composition has gradual variation [33] which changes all over the material volume [26]. The combination of the FGM gradient is related to the composition of the material, which is changed from substance to substance which results separate phases with distinguished chemical structures [33]. Instead these gradual variation results additional properties and functions to the material in different sides of its chemical composition, physical state, and geometrical configuration [26].

The second group of FGMs is the gradients in porosity which is considered an important material ingredient of FGMs [26]. The porosity has the gradual variation through the material's volume [35]. In the manufacturing of functionally graded porosity, both of the size of the porosity and its shape are very essential, especially its shape is of great amount of importance [38] due to the additional properties such as mechanical shock resistance, thermal insulation, and the relaxation of thermal stress [26].

The third one includes graded in microstructure, this category mentions to materials where the surface exhibits a different microstructure compared to the core. These components are basically resulted during the cooling process, thus the heat treatment in these materials has

a significant role. These are applicable in devices where the surface must own wear-resistance. In which the nucleus of the body has different characteristic [33].

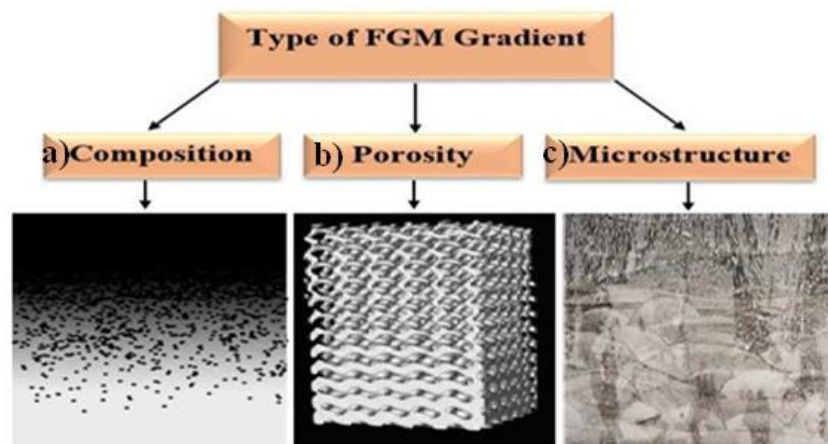


Figure I.12: Classification of FGM based on type of FGM gradients [33].

I.6. Comparison of FGM Materials and Traditional Materials

In general the FGM properties are primarily special and diverse from any material which is formed individually. There are several FGM potential uses which are expected to be increased with the reduction of the cost of material processing and manufacturing processes by these processes improvement [36]. So these materials are advanced composite materials with a non-uniform microstructure. FGM have a dual property of the two raw materials that are mixed together and the component distribution is graduated continuously. For example, one of the FGM that consist of metal and ceramic has the characteristic of thermal conductivity and metal strength in the metal side and high temperature resistivity of the ceramic side [24].

A composite material consists of two or more materials of different types, whose combination performance is better than these components taken separately from such ways to have a material that has coveted properties such as rigidity, mechanical strength, corrosion resistance as well as weight reduction [2]. these materials will collapse under hard working conditions due to a phenomena knows as delamination which means the separation of fibers from the matrix, and the reason is the abrupt transition in composition. This can be occurred, in high temperature application including two metals with various expansion coefficients. Functionally graded materials, delete the abrupt interfaces found in composite material where failure typically begins. It introduces graduated interface rather than the sharp interface in order to produce a smooth transition from one material to another. A distinguishing feature of FGM is there capacity to design the material precisely for specific applications [36].

Since composites are in-homogeneous materials, they have interfaces that is to say contact surfaces between the matrix and the reinforcement , As long as the composite is intact, the two constituents adhere perfectly to each other, And so the interface does not play any particular role. However, the interface plays an important role when the composition undergoes mechanical and starts to crack due to overload, fatigue, ...etc. Indeed, interfaces have the property of deflecting cracks: when a crack propagates in the matrix and reaches the interface (Figure I.13 (a)), usually it does not pass through the latter, so the reinforcements are not damaged. instead, The crack changes direction and follows the interface (Figure I.13(b)). In other words, instead of a sudden break, there is more of a decohesion that is to say, a gradual detachment between the reinforcements and the matrix [4].

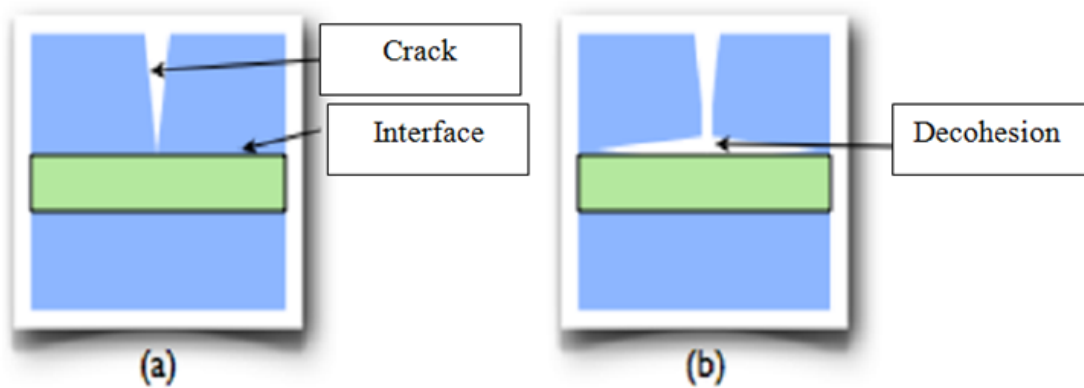
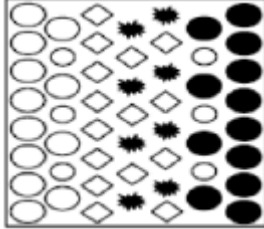
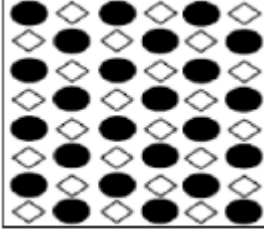


Figure I.13: The role of the interface on the toughness of composites [4].

When a crack reaches the interface (Figure I.14 (a)), it is deflected (Figure I.15 (b)). Rather than abrupt breakup, therefore there is a progressive decohesion of the constituents [4].

Generally, FGMs are materials made up of several layers containing different components such as ceramics and metals. Therefore they are composites with macroscopically inhomogeneous properties. Therefore the continuous change in the composition and in the microstructure of the material distinguishes the FGMs of conventional composite materials as illustrated in table (I-1). These result a gradient which will determine the material properties of the FGMs. in certain cases, we can have an FGM made up of the same material but with a different microstructure [37].

Table I.1: Characteristics of FGM composite materials in comparison with conventional composite materials.

Properties	Mechanical resistance — — — Thermal conductivity — — —		
Structure	Constituent element: Ceramic ○ Metal ● Micro-porosity ○ Fiber ◇		
Material	Example	FGM	NON-FGM

The simplest model illustrating the differences between Property Gradient Materials (FGM) and more conventional materials is shown in Figure (Figure I.14). The plane material (Figure I.14 (a)) composed of a plane characteristic. And the connected material (Figure I.14 (b)) has a boundary on the interface of two materials. FGMs have excellent characteristics that differ from those of composite and bonded planar materials. Therefore, FGMs attract attention in terms of their application in industrial fields since they have a dual property of the two raw materials that are mixed together. And the component distribution is graduated without interruption. For example, one of the FGM which is composed of metal and ceramic has the characteristic of thermal conductivity and metallic strength in the metal side and high temperature resistivity in the ceramic side [38].

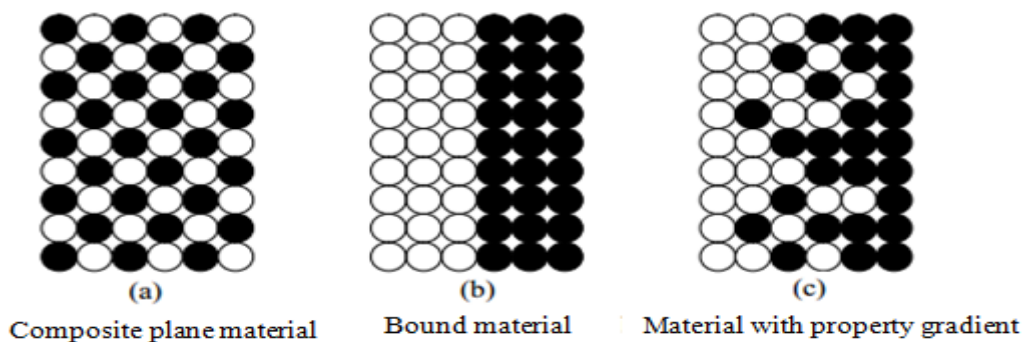


Figure I.14: The component distribution of materials.

Most of “FGMs” are made up of ceramics and metals whose mechanical properties are compared in Table (I.2).

Table I.1: Comparison of the mechanical properties between ceramics and metals.

The high temperature face	Ceramic	<ul style="list-style-type: none"> - Good thermal resistance - Good resistance to oxidation - Low thermal conductivity
Continuity of the material properties from one point to another (intermediate layers)	Ceramic – Metal	<ul style="list-style-type: none"> - Elimination of interface Problems - Relax thermal constraints
The low temperature face	Metal	<ul style="list-style-type: none"> - Good mechanical resistance - High thermal conductivity - Very good tenacity

I.7. Governing laws of the material properties variation of FGM plates

Materials with gradient properties are manufactured by changing the constituents of materials with a non-uniform microstructure which vary gradually without interruption; this can be likened to a stack of an infinite number of layers linked together, and each has its own properties. These connections provide better resistance to breakage, and also excellent hardness on the outside to prevent wear. To describe this variation in volume fractions, researchers use the power function, the exponential function, or the sigmoid function to apply them in the synthesis method used [3].

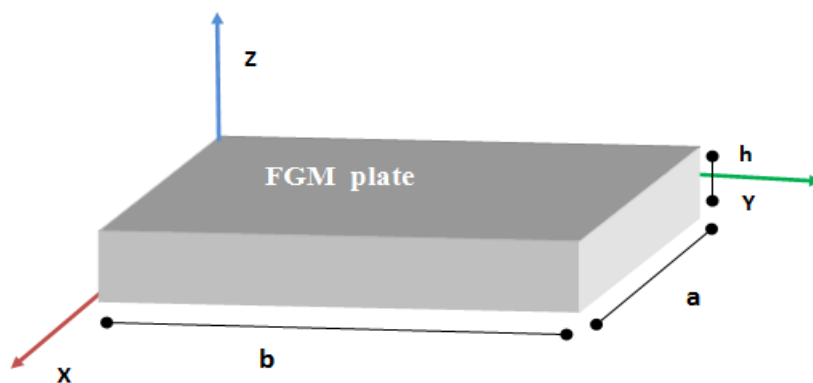


Figure I.16: Geometry of a plate made of materials with gradient properties [3].

I.7.1. Material properties of P-FGM plates

In a P-FGM plate, the volume fraction obtained a power law under the form:

$$V(z) = \left(\frac{z + h/2}{h} \right)^p \quad (\text{I.1})$$

Where:

p : is the material parameter

h : is the plate thickness

z : Presents coordinated according to thickness.

Once the local volume fraction $V(z)$ is defined, the material properties of a P-FGM beam can be determined by the mixture law:

$$E(z) = (E_c - E_m)V(z) + E_m \quad (\text{I.2})$$

E_c and E_m are respectively the Young modulus of the materials constituting the P-FGM plat of the upper surface $z = +h/2$ and the lower surface $z = -h/2$

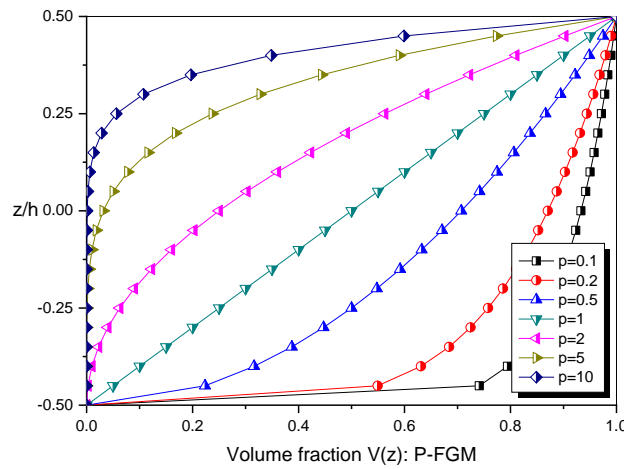


Figure I.17: Volume fraction of the constituents $V(z)$ along the thickness of a P-FGM plate for various values of the power-law exponent p .

We notice that when the Young's modulus increases, the plate becomes very resistant thanks to the ceramic content which is very high, but the resistance of the plate becomes low when we approach the zone where there is a reduction in this content and the increase in that of the metal. It is clear that the Young's modulus changes rapidly near the lower surface for $p > 1$, and increases rapidly near the upper surface for $p < 1$. With ($p = 1$), the variation of Young's modulus becomes linear.

I.7.2. Material properties of S-FGM plates

Chung and chi (2001) [39] defined the FGM plate volume fraction using two power law functions to ensure good stress distribution among all interfaces. The two power law functions are defined by:

$$v_{c1}(z) = \frac{1}{2} \left(\frac{h/2 + z}{h/2} \right)^p \quad \text{for } -h/2 \leq z \leq 0 \quad (\text{I.3a})$$

$$v_{c2}(z) = 1 - \frac{1}{2} \left(\frac{h/2 + z}{h/2} \right)^p \quad \text{for } 0 \leq z \leq h/2 \quad (\text{I.3b})$$

Using the mixing law, the young modulus of the S-FGM plate is calculated by:

$$E(z) = v_{c1}(z)E_c + [1 - v_{c1}(z)]E_m \quad \text{pour } -h/2 \leq z \leq 0 \quad (\text{I.4a})$$

$$E(z) = v_{c2}(z)E_c + [1 - v_{c2}(z)]E_m \quad \text{pour } 0 \leq z \leq h/2 \quad (\text{I.4b})$$

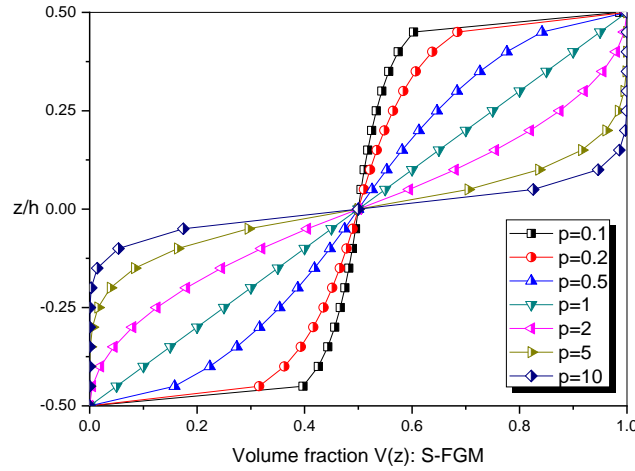


Figure I.187: Volume fraction of the constituents $V(z)$ along the thickness of a S-FGM plate for various values of the power-law exponent p .

I.7.3. Material properties of E-FGM plates

Several researchers adopted the exponential function to predict the mechanic behavior of FGM structures. For a FGM structure of uniform thickness h , the typical properties of the material at any point at a z distance from the reference surface are given in the form:

$$V(z) = e^{p \left(\frac{z+1}{h+2} \right)} \quad (\text{I.5a})$$

$$E(z) = E_m V(z) \quad (\text{I.5b})$$

The variation of Young's module through the thickness of the E-FGM plate is shown in (Figure I.18).

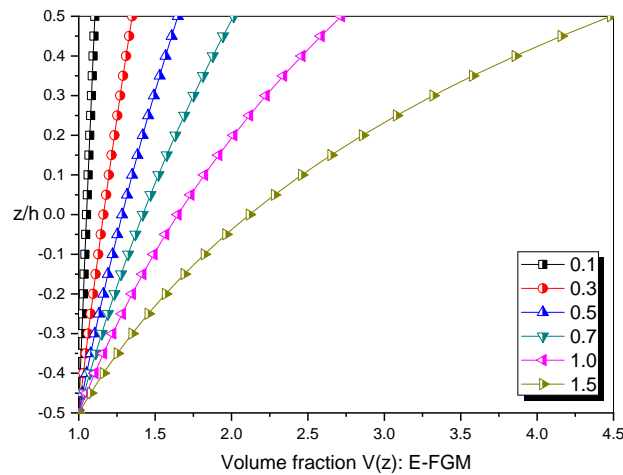


Figure I.19: Volume fraction of the constituents $V(z)$ along the thickness of an E-FGM plate for various values of the power-law exponent p .

From Figure (I.18), we notice that the increase in Young's modulus is proportional to the increase in the quantity of ceramic relative to that of metal while moving towards the upper end of the plate.

I.8. Application Area

Due to the unique graded materials properties, FGMs have a wide range of application thanks to their very important potential use [2].

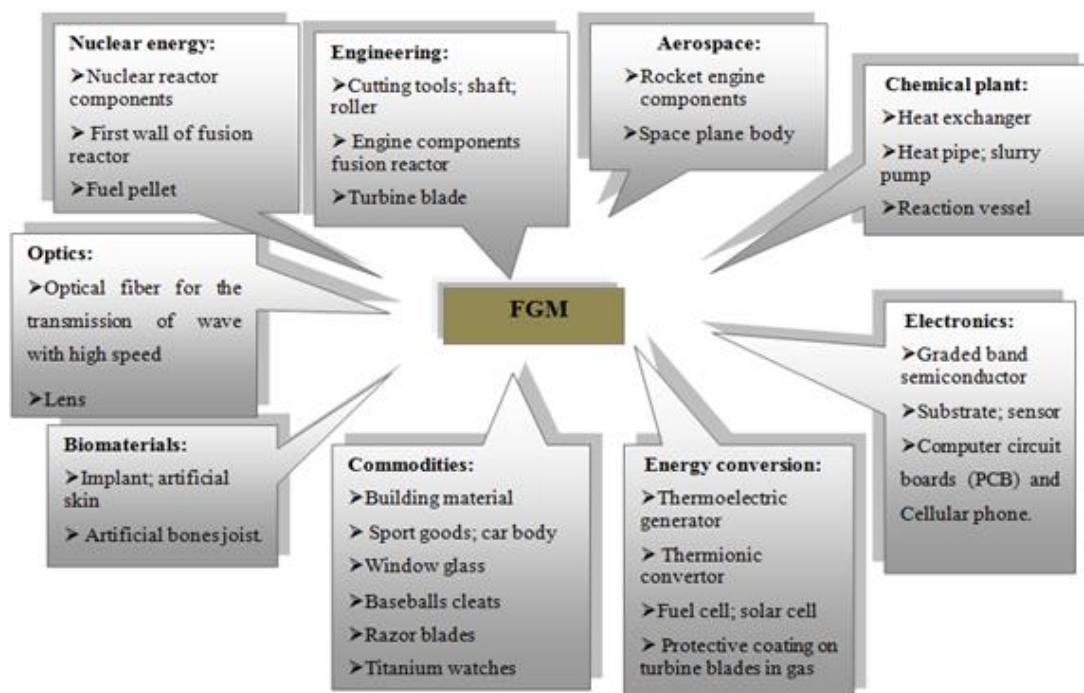


Figure I.20: Various fields of Application of FGMs [21].

I.8.1. Thermal barrier (Coating)

Thermal barrier coatings are widely applicable in many environments that have excessive heat in order to reduce thermal stresses because of the differences of the properties within the material to avoid the chances of the failures of the component [26].

I.8.2. Defense

The primary property of functionally graded material is the ability to inhibit crack propagation [21] and that makes it useful in defense industry in applications such as bulletproof vests, traditional Japanese sword and armor as well as the body of bulletproof vehicles [25].

I.9. Advantages and disadvantages of FGMs

I.9.1. Advantages of FGM

FGMs provide several properties in different fields such as [40]:

- Mechanical strength by various materials such as the metal
- High tensile strength
- The best penetration resistance
- Very good solidity, hardness and rigidity
- Good protective properties and good thermal conductivity

I.9.2. Disadvantages of FGMs

The manufacture of functionally graduated materials breaks a great obstacle and this because of the mismatch between the different properties of the materials used; we can evoke the size of the particles, the morphology and the temperature, etc [2].

High porosity and low adhesion between the different constituents

The manufacture of this type of material must be under conditions such as a protective atmosphere or low pressure but unfortunately these two processes are very expensive.

I.10. Conclusion

This review of the literature allowed us to define functional gradient materials “FGM”, the history of their development, their definitions and their areas of application and give an overview of their effective properties which vary gradually and continuously from one face to another through the thickness. Further the spatial and progressive variation of the properties of these materials makes it possible to create innovative structures; the different mixing laws

were presented which manage the variation of the material properties of said materials, namely: the power law function (P-FGM), the exponential function (E-FGM) and the sigmoid function (S-FGM). These laws are used to describe the variation of volume fractions.

■ *Chapter II*

The different theories of FGM plates

Chapter II

The different theories of FGM plates

II.1. Introduction

Laminates are two-dimensional elements, of planar shapes with large dimensions in relation to their thickness noted (h). They can be found in various fields of industry. To this end, the designer must carefully study their behavior and states limits in various conditions of use and environmental conditions in order to avoid failures or accidents that may arise with the aim of obtaining exact results relating to the study of the static and dynamic behavior of the plates [3], to characterize the analysis model, different hypotheses are necessary [4]:

- Thin plates with small deflections (Kirchhoff-Love) where the energy contribution of the shear effect is neglected.
- Thin plates with large deflections (Karman).
- Moderate or thick plates (Mindlin-Reissner) where the contribution energy of the shear effect is preserved.

II.2. Definition of the plates

A plate is defined as solid object, limited by two parallel flat surfaces, whose lateral dimensions which are the width and length (in the case of rectangular plate) and the diameter (in the case of a circular plate) are large compared to the distance between the flat surfaces which is the thickness of the plate (h), and it is subjected to bending deformation and stretching loads [41].

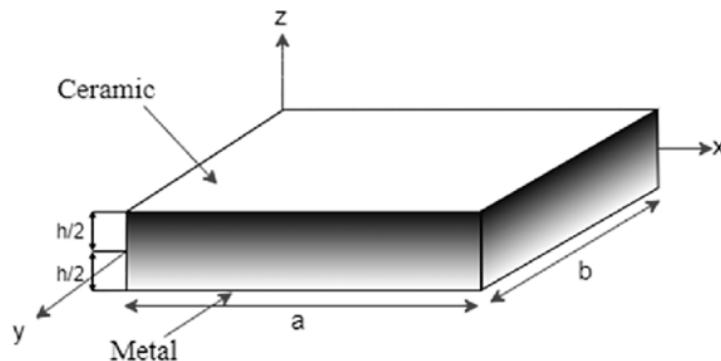


Figure II.1: Model of an FGM plate.

Plates can be divided into two categories which are: thin plates ($a/h > 20$) and thick plates [23].

Plate theory is based on the following assumptions [4]:

- The plate is small in thickness compared to the other dimensions. It has a medium plane also called neutral plane.
- Plane stress hypothesis: in the relation of mechanical behavior of the plate, the normal stress in the transverse direction σ_z is small; therefore it is negligible compared to the stresses belonging to the plane of the plate.
- The hypothesis of plane anisotropy of the plate.

II.3. Different types of plates

The plates can be classified into three categories:

- Isotropic plates,
- Orthotropic plates,
- Anisotropic plates.

II.3.1. Isotropic plates

Isotropic plates are defined by two elastic parameters (respectively the modulus of elasticity and Poisson's ratio) and they are made of an isotropic material, for example (steel, concrete) [3]. If a material has an infinite number of planes of symmetry, it is said to be isotropic. And their cross-section is homogeneous, they are found in common civil constructions (construction, engineering) [24].

II.3.2. Orthotropic plates

Their elastic properties are different in two perpendicular directions. This aspect can be found either natural (wood) or technical (recast slabs). The behaviors of these slabs are defined by four elastic parameters and are often used in: naval construction, chemical industry tanks, buildings and engineering structures [24].

II.3.3. Anisotropic plates

Anisotropic plates are plates whose elastic properties are different in all directions. Nine elastic parameters are enough to become them. They are often made of composite materials and are mainly used in industry [3].

II.4. Application area

The field of use of plate is very widespread in all fields, in particular in the field of civil engineering where they are used in simple constructions (housing) or works of art and it exists

in different forms, including circular and rectangular and other shapes depending on the quality of the work, as shown in the photos below [24].

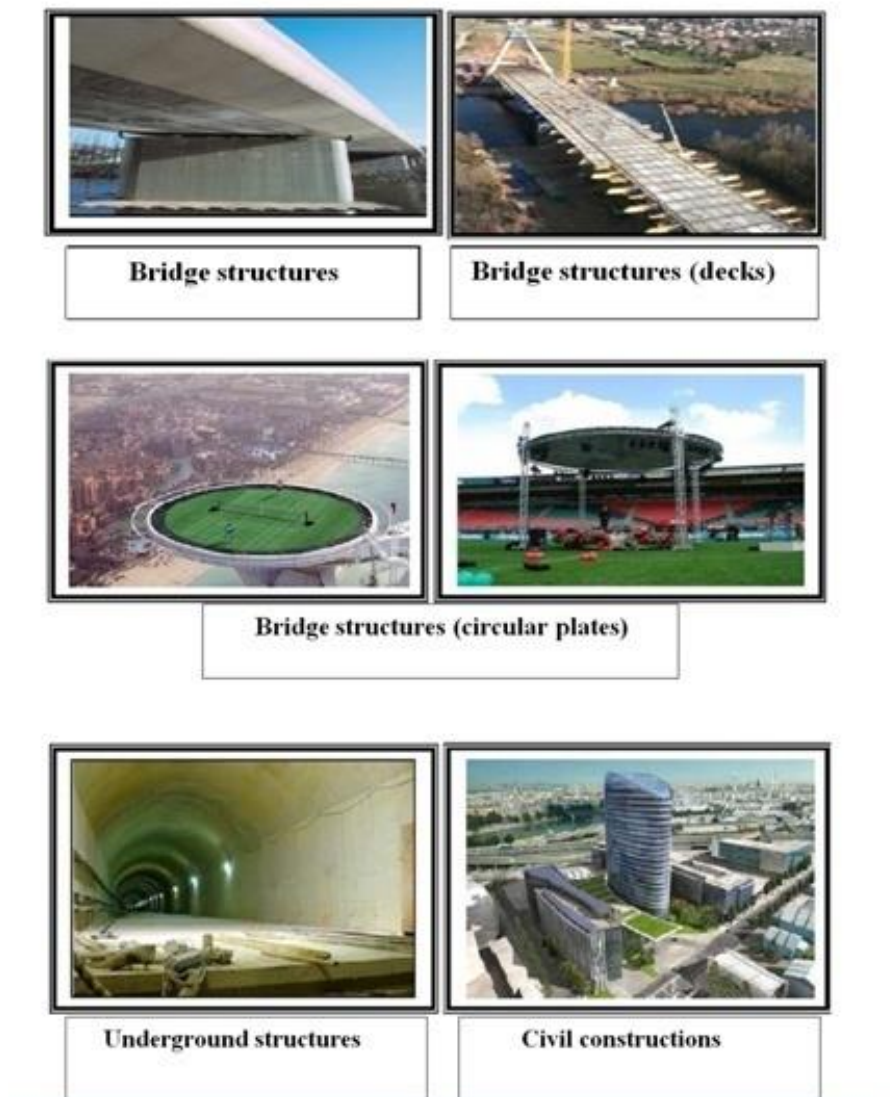


Figure II.2: Application Area [24].

II.5. Different types of theories

In order to be able to study a behavior whatever is static or dynamic structures having FGM beams and plates as structural elements in the elastic domain, It is necessary to choose the appropriate theory that can correctly describe their behavior (static and dynamic) [27].

The different existing 2-D elasticity theories can therefore be classified into four main categories: classical theories of thin plates (Kirchhoff-Love theory), first order plate theory (Mindlin-Reissner theory) applicable to moderately thick plates, higher order theory applicable to thick plates (like Reddy's) came to improve the hypotheses of classical and first

order theories when the thickness of the plate becomes important. And theory based on 3-D elasticity theory which makes no restrictive hypothesis on the displacements of the plate.

Plate analysis is a three-dimensional problem. Almost all the theories developed have had as their main object the reduction of the 3-D problem to a 2-D problem by using simplifying assumptions concerning the kinematics of deformations and the state of stresses through the thickness [4].

II.5.1. Bi-dimensional theories

II.5.1.1. Classical plate theory (CPT)

The small deflection of bending of thin plate generated by the shear deformations remains negligible compared to the deflection generated by the curvature of the plate. It is noted that this theory is not applied in the case of moderately thick or very thick plates [27].

a. The hypotheses of the CPT theory

- The plate is of small thickness compared to the other dimensions (the length a and the width b); slenderness ratio $h/a \geq 20$. It has average plane [30];
- The straight sections, initially normal to the average plane, remain flat and normal to the average plane after bending [23]. Therefore the effects of transverse shear deformation are negligible [30];
- The thickness is low; consequently, the stresses in the thickness direction are assumed to be zero ($\sigma_z = 0$) [3];
- Normal line in the mean plane (average plane) of a plate remains perpendicular after deformation [2]; all of the notations are schematized in figure (II.1);
- This theory neglects the transverse shear effect and the effect of axial deformation in the transverse direction [35], the deformation of the plate is essentially due to bending and in-plane deformation (Figure II.3) [41]; which limits the validity of this theory to thick plates.

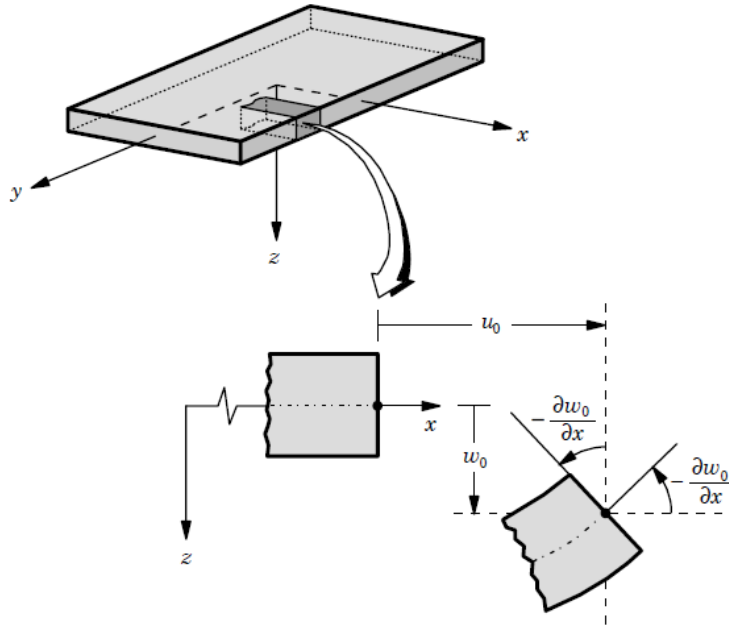


Figure II.3: Schematization of plate deformations according to the hypotheses of classical theory (CPT) [41].

b. The displacement field

Under these assumptions, the field of displacements of a point of coordinates (x, y, z) is written [41]:

$$\begin{aligned}
 u(x, y, z) &= u_0(x, y) - z \frac{\partial w_0(x, y)}{\partial x} \\
 v(x, y, z) &= v_0(x, y) - z \frac{\partial w_0(x, y)}{\partial y} \\
 w(x, y, z) &= w_0(x, y)
 \end{aligned} \tag{II.1}$$

where u_0, v_0, w_0 are the displacements components along the average plane of the plate x, y and z axes, respectively.

$\partial w_0(x, y)/\partial x$ and $\partial w_0(x, y)/\partial y$ represent the rotation of the normal fiber around the axes x and y , respectively.

II.5.1.2. First shear deformation theory (FSDT)

This theory is considered an improvement on the classical theory of thin plates (Kirchhoff theory), compared to the previous theory, the first-order shear deformation theory takes into account the transverse shear effect [2].

This theory assumes that straight sections initially normal to the neutral plane remain flat and not necessarily normal to it after deformation because of the transverse shear effect (Figure II.4) [34].

The correction factor is necessary required in this theory for two reasons:

- FSDT gives a constant value of transverse shear deformation through the thickness of the plate and also a false description of the field of tangential stresses, therefore it is necessary to introduce correction factors of Shear in the form of dimensionless quantities [3].
- Since first order plate theory (FSDT) does not satisfy the boundary conditions at the upper and lower surfaces of the plate (non-zero tensile stresses), through-thickness shear and the correction factor value depends on the geometry of the plate, the variation of the Poisson's ratio across the thickness, the applied loading and the imposed boundary conditions [4].

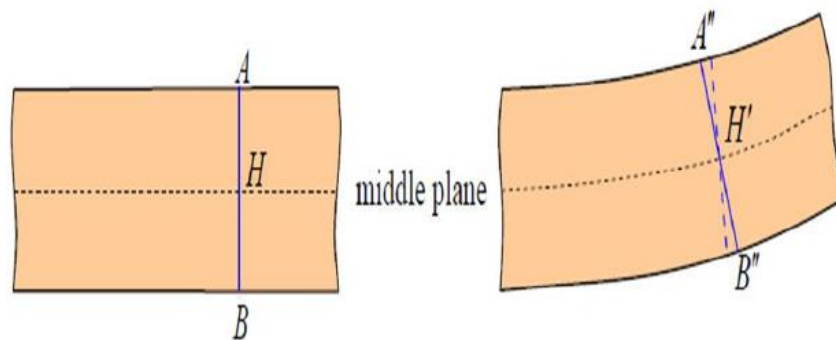


Figure II.4: Deformation with transverse shear (first degree schema) [4].

a. The displacement field

In this theory the normal remains straight but not perpendicular to the average surface (due to the effect of transverse shear) [3]. So the displacement field is as follows [30]:

$$\begin{aligned}
 u(x, y, z) &= u_0(x, y) + z\phi_x(x, y) \\
 v(x, y, z) &= v_0(x, y) + z\phi_y(x, y) \\
 w(x, y, z) &= w_0(x, y)
 \end{aligned}
 \tag{II.2}$$

Where:

u_0, v_0, w_0 are the membrane displacements that is to say they are displacements along the coordinate axes x, y and z of a point on the average plane (plane $z = 0$).

ϕ_x and ϕ_y are the rotations of the normal to the cross section with respect to the y and x axes, respectively.

with:

$$\begin{aligned}\phi_x &= -\frac{\partial w_0}{\partial x} + \gamma_{xz}, \\ \phi_y &= -\frac{\partial w_0}{\partial y} + \gamma_{yz}\end{aligned}\quad (\text{II.3})$$

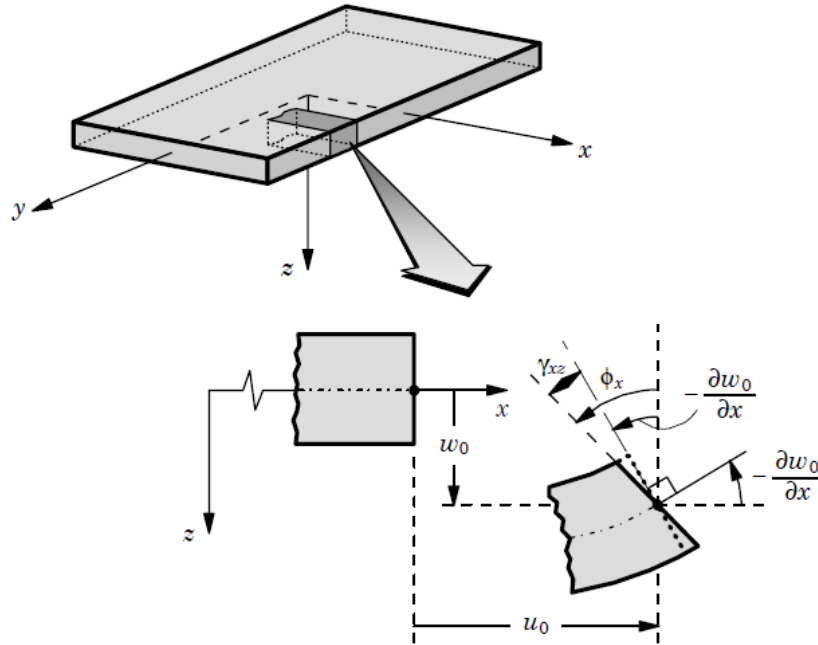


Figure II. 5: Schematization of deformations of first order plate theory [41].

II.5.1.3. High-order shear deformation theory (HSDT)

This theory is an evolution of the classical plate theory (CPT) and that of the first order (FSDT). It is based on a non-linear distribution of transverse shear strains across the plate thickness (parabolic distribution). The effects of transverse shear deformation and/or transverse normal deformation are taken into account. These models do not require correction factors [34]. By analyzing studies developed by several authors we find that these higher order theories are more precise than the CPT and FSDT theories, this precision is the result of the introduction of several additional unknowns [3].

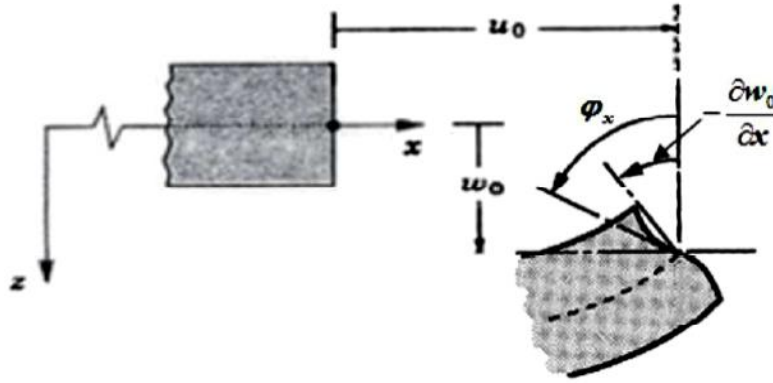


Figure II.6: Schematization of deformations in the case of higher-order plate theory [2].

a. The hypotheses of the HSDT theory

The hypotheses which are the basis of the development of this theory are [4]:

- The displacements are small compared to the thickness of the plate;
- The cross sections, initially planar and normal to the average plane, do not necessarily remain planar and normal to it after deformation;
- The axial deformation in the transverse direction is generally not negligible;
- Normal stresses in the transverse direction are generally not negligible.

b. The field of displacement

Most theories of deformation in High-order shear are based on approaches from Reissner [42], Mindlin [43] and Ambartsumian [44], which has the following displacement:

$$\begin{aligned}
 u(x, y, z) &= u_0(x, y) - z \frac{\partial w_0(x, y)}{\partial x} + f(z)\varphi_x(x, y) \\
 v(x, y, z) &= v_0(x, y) - z \frac{\partial w_0(x, y)}{\partial y} + f(z)\varphi_y(x, y) \\
 w(x, y, z) &= w_0(x, y)
 \end{aligned} \tag{II.4}$$

In which $f(z)$ represents the shape function determining the distribution of transverse stresses and deformations according to thickness.

In classical plate theory (CPT) the displacement field is obtained by setting $f(z) = 0$ [34].

The first order shear deformation theory (FSDT) is obtained by setting $f(z) = z$ [27].

Below are some important contributions to the development of higher-order models that have distinguished themselves in the literature and differ by the function of $f(z)$ forms [3]:

- **The approach of Reddy** [45]

In this Reddy model, we see that there is a good approximation for the transverse and parabolic shear stresses in the thickness with a membrane displacement field which is cubic. And the boundary conditions on the free surfaces are satisfied [45]:

$$f(z) = z \left[1 - \left(\frac{4z^2}{3h^2} \right) \right] \quad (\text{II.5})$$

- **The approach of Touratier** [46]

Known as sinusoidal shear deformation theory (SSDT) which is proposed by Touratier, aims to model the distribution of shear stresses through the thickness, it does not use polynomial function [46]:

$$f(z) = \left(\frac{h}{\pi} \right) \sin \left(\frac{\pi z}{h} \right) \quad (\text{II.6})$$

The transverse shear stresses determined by the models (sine) take a cosine shape across the thickness of the plate. The accuracy of this model compared to the exact solution is better than Reddy's theory [4].

- **The approach of Karama** [47]

The exponential version of the high order shear deformation theory (The exponential shear deformation plate theory ESDPT) developed by Karama in 2003 as follows [47]:

$$f(z) = ze^{-2\left(\frac{z}{h}\right)^2} \quad (\text{II.7})$$

Other high-order theories (refined) have been developed using different transverse shear functions [3] in their field of displacements with the unified form is written according to formula (II.4) where the function $f(z)$ is the function of the pile form the distribution of shear deformations and stresses through the thickness of the plate. We group in Table II.1 below the different transverse shear functions as well as a comparison between the different models. The high-order models and their derivatives are also represented by Figures II.7 and II.8.

Table II.1: Different shear functions of isotropic plate theories and FGM as well as a comparison between the different models [4].

Theory	Titled	Shape function	Distribution of τ_{xz} and τ_{yz}	Correction function	Validity
Kirchhoff [48]	CPT	$f(z) = 0$	/	/	Thin plate
Mindlin [43]	FSDPT	$f(z) = z$	Constant	Required	Thin and medium thick plates
Ambartsu- mian [44]	HSDPT	$f(z) = \frac{z}{2} \left(\frac{h^2}{4} - \frac{z^2}{3} \right)$	Quadratic	Not required	Thin and medium thick plates
Reissner [42]	HSDPT	$f(z) = \frac{5}{4} z \left(1 - \frac{4z^2}{3h^2} \right)$	Parabolic	Not required	Thin and thick plates
Touratier [46]	SSDPT	$f(z) = \frac{h}{\pi} \sin\left(\frac{z}{h}\right)$	Trigonométrique	Not required	Thick plates
Soldatos [49]	HySDPT	$f(z) = h \sinh\left(\frac{z}{h}\right) - \frac{4z^3}{3h^2} \cosh\left(\frac{1}{2}\right)$	Hyperbolique	Not required	Thick plates
Karama [47]	ESDPT	$f(z) = ze^{-2\left(\frac{z}{h}\right)^2}$	Parabolic	Not required	Thick plates
Reddy [45]	PSDPT	$f(z) = z \left(1 - \frac{4z^2}{3h^2} \right)$	Parabolic	Not required	Thick plates
Aydogdu [50]	ESDPT	$f(z) = z3^{\frac{-2(z/h)^2}{\ln 3}}$	Exponentielle	Not required	Thick plates
Zenkour [51]	TSDPT	$f(z) = h \sinh\left(\frac{z}{h}\right) - \frac{4z^3}{3h^2} \cosh\left(\frac{1}{2}\right)$	Parabolic	Not required	Thick plates
Present	PSDPT	$f(z) = \frac{7}{4} z - \frac{7z^3}{3h^2}$	Parabolic	Not required	Thick plates

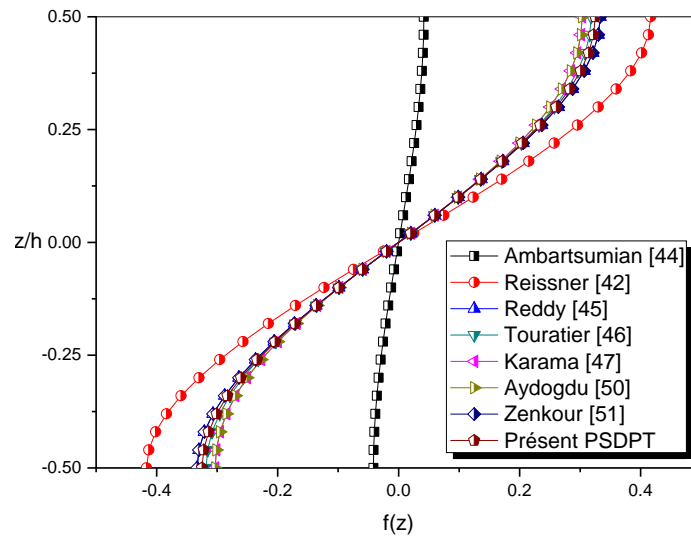


Figure II.7: Variation of the shear function $f(z)$ of different high-order models across the plate thickness.

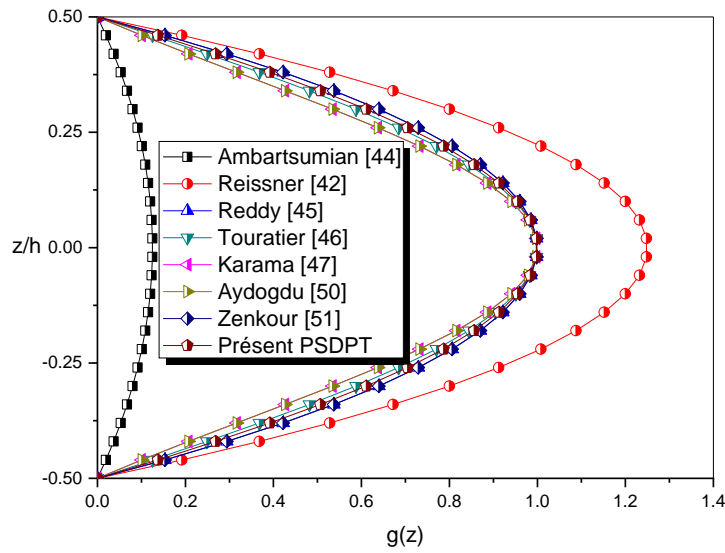


Figure II.8: Variation of the shear function derivative $g(z)$ of different high-order models across the beam thickness.

II.5.1.4. Refined plate theory (RPT)

Refined Plate Theory (RPT) was developed by Shimpi [52] for the isotropic FGM plates with reduction in number of unknowns. It is based on both the effects of shear deformation and thickness stretching without requiring a shear correction factor and gives a parabolic shear distribution across the thickness of the plate [3]. The number of unknowns is four u_0, v_0, w_b, w_s contrary to classical theories which count five $u_0, v_0, w_0, \phi_x, \phi_y$ [34]. It contains only two variables which gives only four unknowns to be determined instead of five in the classic case. Several researchers have demonstrated the reliability of this theory [27]; they applied this theory in the case of bending of FGM plates in the static case and in the case of buckling of orthotropic plates.

a- The displacement field

The displacement field of this theory is therefore written [53]:

$$\begin{aligned} u(x, y, z) &= u_0(x, y) - z \frac{\partial w_b(x, y)}{\partial x} - f(z) \frac{\partial w_s(x, y)}{\partial x} \\ v(x, y, z) &= v_0(x, y) - z \frac{\partial w_b(x, y)}{\partial y} - f(z) \frac{\partial w_s(x, y)}{\partial y} \\ w(x, y, z) &= w_b(x, y) + w_s(x, y) \end{aligned} \quad (\text{II.8})$$

with:

u_0, v_0 are the components of the displacement field in the x and y directions.

w_b, w_s are the bending and shear components of the transverse displacement .

$f(z)$ is the transverse shear function.

II.5.1.5. higher-order shear and normal deformation theory (quasi-3D)

In this theory, we divide the transverse displacement into three constituents which are the bending, shearing and stretching effect of the thickness of the plate, many researchers proposed a hyperbolic shear deformation theory in quasi-3D for bending and free vibration of FGM plates or the number of unknowns to be determined is five displacements and meets the boundary conditions of traction which must be zero at the surface of the plates without requiring a shear correction factor [3]. This theory is proposed with a number of unknowns which is reduced to four for FGM plates [27]; it was developed to study medium thickness and very high thickness plates [34]. The quasi-3D hyperbolic theory uses only five variables unknowns to determine the responses to quadruple coupled vibrations (shear axial-bending-stretching) [3]. By further simplifying the assumptions of Zenkour theory [54] on a new

quasi-3D with four unknowns by combining both stretching and shear deformation effects without requiring a shear correction factor.

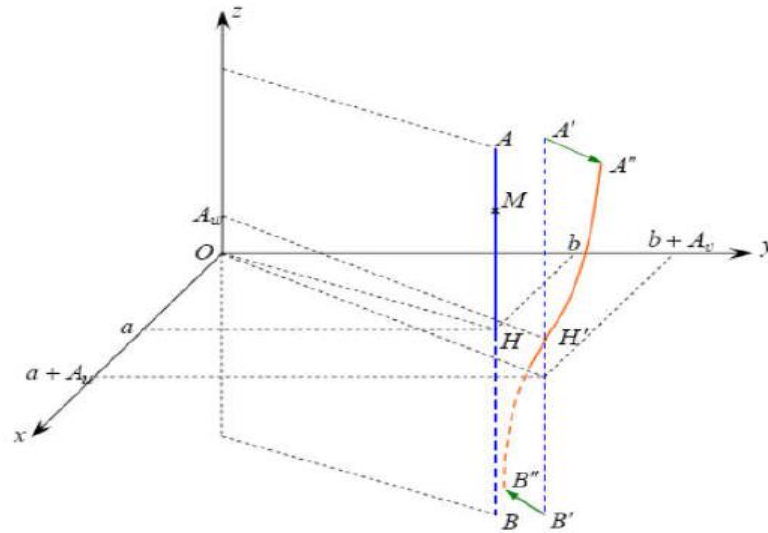


Figure II.9: Presentation of stretching effect through thickness [3].

Therefore the displacement field in this theory is presented as follows [34]:

$$\begin{aligned}
 u(x, y, z) &= u_0(x, y) - z \frac{\partial w_b(x, y)}{\partial x} - f(z) \frac{\partial w_s(x, y)}{\partial x} \\
 v(x, y, z) &= v_0(x, y) - z \frac{\partial w_b(x, y)}{\partial y} - f(z) \frac{\partial w_s(x, y)}{\partial y} \\
 w(x, y, z) &= w_b(x, y) + w_s(x, y) + g(z)\varphi(x, y)
 \end{aligned} \tag{II.9}$$

where $\varphi(x, y)$ is an additional displacement which takes into account the stretching effect.

$g(z)$ is a transverse shear function with:

$$g(z) = 1 - f'(z) \tag{II.10}$$

II.5.2. Three-dimensional theory (3D) elasticity

Three-dimensional elasticity context is able to conduct the dynamic and static studies on FGM plates. In the first place we should note that no hypotheses are adopted on the displacement field [24]. The study of the behavior of functionally graduated plates with respect to mechanical and thermal loadings remains a three-dimensional problem so the use of three-dimensional (3D) elasticity theories can be very useful. Over the past twenty years, many researchers have been interested in 3D elasticity theories in order to develop more accurate solutions for the mechanical behavior of FGM plates and validate the results of

different analytical models [27]. Using of the space state method that Alibeigloo [55] performed a bending analysis of FGM plates under thermal and mechanical loads. In the years that followed quite a lot of work was recorded as part of the static study under thermal and mechanical loads of FGM plates using theories of three-dimensional (3D) elasticity. Vel and Batra [56] were also interested in three-dimensional vibration studies of FGM plates using the power series method for plates simply supported in FGM [27]. Then Aydogdu and Uymaz [57] presented exact solutions using 3D theories for free vibration of FGM plates with different boundary conditions. The 3D elasticity theory and the quadratic difference method were used to obtain proper frequencies. Other dynamic studies conducted for functionally graded plates [23].

It can be seen that the advantage of solutions based on the three-dimensional (3D) elasticity theory is that it has no restrictive hypothesis [30].

II.6. Layered approach

These approaches are intended precisely to better describe the interface effects for conventional composites materials; also this approach is applicable for FGM materials. Thus different models resulting from the approach per layer were proposed [37]. The multilayer is subdivided into substructures (corresponding in fact to each layer or each set of layers). We apply to each substructure a theory of the first order or a higher order model, imposing a displacement field verifying the continuity at the interfaces between the different layers [31]. Models of this type are relatively expensive (the order of the behavioral equations depends on the number of layers), but they make it possible to obtain more precise results, particularly with regard to the calculation out-of-plane stresses [40].

Generally, the models resulting from the layer approach can be classified in two groups [37]:

- Zig-zag models or kinematics a priori satisfy the contact conditions are independent of the number of layers;
- Discrete layer models where each layer is considered as a plate by imposing the conditions of continuity in displacements or stresses on the interfaces.

II.6.1. Zig-Zag models

In order to reduce the number of unknown parameters, Di sciuva [58] is the first to propose the zig-zag model. In this model, the movements membranes are the results of the superposition of the global displacement field of a first-order theory and a zig-zag function (with the use of the Heaviside function). There zig-zag function gives a contribution from

membrane displacements which are continuous in z but its first derivative is discontinuous at the interface (see Figure II.10). Transverse deformations are therefore discontinuous and the continuity of the transverse shear stresses at the interfaces is ensured [31].

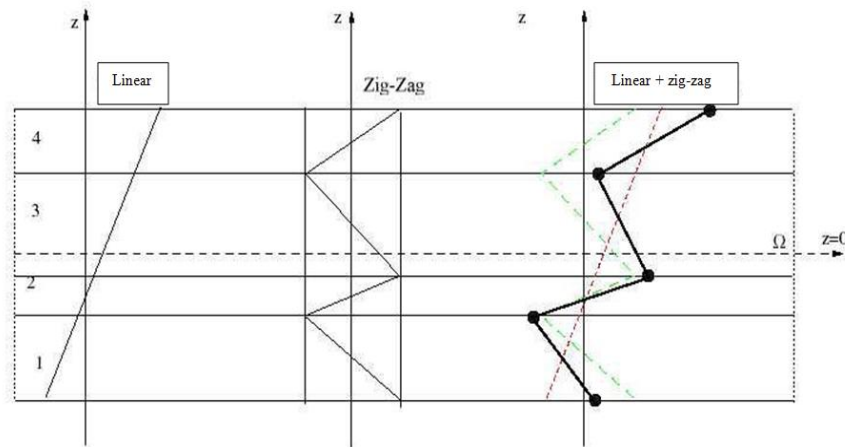


Figure II.10: Displacement fields of first-order zig-zag models [31].

The main advantage of the displacement field of zig-zag models lies in the good modeling of the distortion of the normal of the deformed surface, as well as in the verification of continuity conditions, without increasing the number and fundamental equations order of first order theory. The use of coefficients of correction for transverse shear is avoided [59]. Several authors have carried out significant improvements for the zig-zag model. The main improvement is the introduction of a non-linear distribution of displacements. We superimpose the zig-zag field (linear per piece) to a higher order-displacement field (often cubic) (see Figure.II.11). Compatibility conditions are met on upper and lower surfaces of plates to reduce the number of parameters [36].

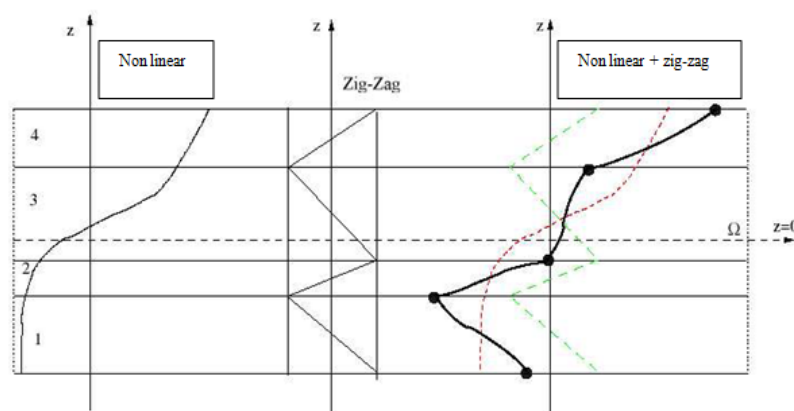


Figure II.11: Displacement fields of higher order zig-zag models [40].

Many researchers have combined the sine function with the zig-zag function to refine the effects of shear and the exponential model with the effect zig-zag for a richer cinematic [43].

The numerical results of all this work show that the zig-zag model ensures a good compromise between the precision of the solutions and the calculation cost. However, the zig-zag models have validation limits in delamination analysis. In fact, nothing physical leads us to think that these somewhat artificial models can predict delaminations, for example [31]. The calculation of transverse shear stresses by the constitutive equations of zig-zag models becomes less precise when the slenderness ratio decreases. Another disadvantage of zig-zag models, just like higher order models are the requested type continuity which complicates their digital implementation [37].

II.6.2. Discrete layer models

Discrete layer models adopt a finer approximation of the following fields the thickness of the multilayer than higher order or zig-zag plate models since they propose a kinematics per layer rather than a global kinematics (see Figure II.12). In fact, with discrete layer models, the multilayer is represented by a set of plates (2D objects) coupled by interface forces. The conditions of continuity interfaces are ensured. The number of unknown parameters depends on the number of layers of the composite plate [31].

The fundamental equations by layer are obtained using the principle of virtual works. The boundary conditions are also given per layer [40]. Alternatively; many researchers use an approximation of the stress fields by layer or a mixed kinematic stresses. Thus they use a stress field whose transverse shear component is quadratic per layer and the displacements are considered cubic per layer and continuous at the interfaces. The stress field is constructed in the form of a product of functions with separate variables, by layer, from the balance of forces and moments. The plane stresses are assumed to be constant depending on the thickness. In, the stress functions are used per layer to determine the inter-laminar stresses. They are approximated by polynomial ways in the thickness [31].

We now move on to a family of particular discrete layer models, the multi-particle models. The local model was built from the Hellinger-Reissner variational formulation and a polynomial approximation of the stress fields per layer. The polynomials are of the first degree for membrane stresses, quadratic for shear stresses and therefore cubic for normal stresses [40].

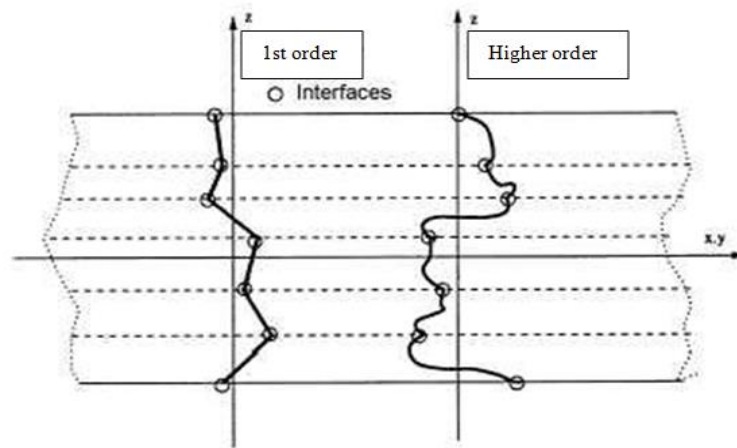


Figure II.12: Fields of movement of discrete layer models, approach cinematic [37].

The Hellinger-Reissner variational formulation restricted to the approximations of these stress fields leads to a multilayer kinematics with $7n$ fields in (x, y) , n being the number of layers of the plate. These kinematic fields contain components corresponding to second order moments which do not have a very clear physical meaning [37]. The mixed Hellinger-Reissner formulation makes it possible to deduce the generalized linear elastic behavior of the model. This model poses some difficulties in terms of boundary conditions and remains quite heavy given the high number of kinematic fields involved. This model was the starting point for a set of works carried out at ENPC whose objective is to propose a series of simplifications making it possible to reduce costs while maintaining a good level of predictability [31].

II.7. Conclusion

In this chapter we have presented the different existing theories for studies of functionally graded material plates FGM which are: the classical theory (CPT) of Love-Kirchhoff used to study the thin plates, first order shear deformation theory (FSDT), high order shear deformation theory (HSDT), the refined theory of deformation (RPT), with respect to quasi-3D shear deformation theory and high-order shear deformation theory (HSDT) they will be the subject to study the static response of thick plates with a functional gradient and we have mentioned to the different theories of the plates, namely: the equivalent single approach, the layer approach and the asymptotic development approach.

We conclude:

- The use of these theories depends on the thickness of the plate.

- The equivalent single-layer approach is better suited for FGM materials because there is no abrupt change in mechanical characteristics unlike conventional composites where delamination is a problem that should not be ruled out.
- Taking into account transverse shear is necessary for a more accurate study.

■ *Chapter III*

**Theoretical approach for bending analysis
of thick exponentially graded plates**

Chapter III

Theoretical approach for Bending analysis of Thick exponentially graded plates

III.1. Introduction

Several studies which have the ability to predict the response of FGM plates subjected to mechanical loads were carried out to analyze the behavior of the plates however it is quite limited [24]. After aforementioned chapter that involves the results of research on some theories of FGM plates, we are going to focus in this chapter on the bending analysis of thick exponentially graded plates proposing a refined higher order theory of shear deformation which takes into consideration the transverse shear effect of FGM plates, which their material properties vary through the thickness according to an exponential function (E-FGM). Unlike conventional refined shear deformation theories, this theory contains only four unknowns.

III.2. Mathematical formulation of present approach

III.2.1. Exponentially graded plate model

As we aforementioned before we deal in our study with a rectangular plate of three dimensions (the length a , the width b , and the uniform thickness h) made of functionally graded materials which are the ceramic and the metal, and these dimensions are defined with respect to a rectangular Cartesian coordinate system (O, x, y, z) , as illustrated in Figure III.1. In the present analysis it is assumed that the Poisson ratio, ν to be constant, contrary, the effective material properties (such as Young's modulus E and mass density ρ), are assumed to vary only across the thickness of the plate in exponential form according to the volume fractions of the constituents (see Figure I.18) and that leads to the following equation:

$$E(z) = E_m V(z), \quad V(z) = e^{p\left(\frac{z}{h} + \frac{1}{2}\right)} \quad (\text{III.1})$$

In which E_m mentions to the metal-rich property (bottom surface) that is related to the exponentially graded plate. Whereas, p is the power-law exponent that controls the material variation profile across the thickness of the EG plate.

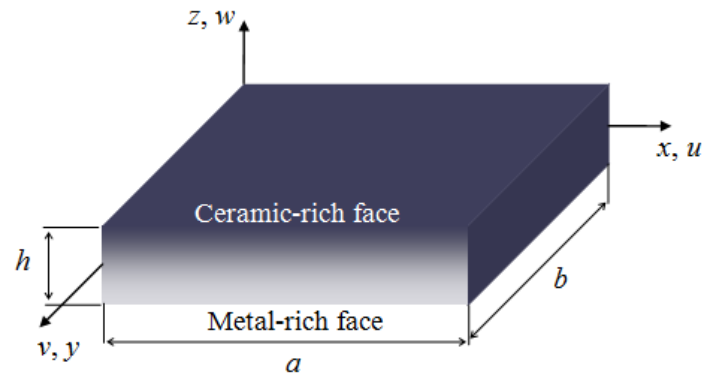


Figure III.1: Geometry of an exponentially graded plate model.

III.2.2. Theoretical formulation assumptions

The kinematic hypotheses which are the basis of the mathematical formulation of the present shear deformation theory are as follows:

1. In relation to bending terms, The axial displacements according to the x and y -directions are considered as the classical beam theory and shear components integral;
2. The transverse displacement according to the z -direction is only contained of the transverse component;
3. The theory involves four independent unknown variables;
4. The theory investigated both of the parabolic distribution resulted from transverse shear stress through the plate thickness and meeting the boundary conditions without requiring the shear correction factor;
5. The normal strain effect is negligible.

III.2.3. Kinematic and constitutive relations

For sake of simplicity, the present study aims to establish a new kinematics with only four unknown variables to predict the static behavior of the exponentially graded plates rather than the conventional refined shear deformation plate theory that has been previously proposed by Mantari and Guedes Soares [59] which its displacement field has five unknowns based on some further simplifying assumptions.

It is worth noting that the displacement field of the conventional refined shear deformation theory is introduced as illustrated in the following equation:

$$\begin{aligned}
u(x, y, z) &= u_0(x, y) - z \frac{\partial w_0(x, y)}{\partial x} + f(z) \varphi_x(x, y) \\
v(x, y, z) &= v_0(x, y) - z \frac{\partial w_0(x, y)}{\partial y} + f(z) \varphi_y(x, y) \\
w(x, y, z) &= w_0(x, y)
\end{aligned} \tag{III.2}$$

Where $u_0(x, y)$, $v_0(x, y)$, $w_0(x, y)$, $\varphi_x(x, y)$, and $\varphi_y(x, y)$ are the five unknown displacement functions of the mid-plane of the plate. Hence, $f(z)$ is the shape function that controls the distribution of the transverse shear strains and the stresses with respect to the plate thickness. By supposing that:

$$\begin{aligned}
\varphi_x &= \int \theta(x, y) dx, \\
\varphi_y &= \int \theta(x, y) dy
\end{aligned} \tag{III.3}$$

The new displacement field of the proposed PSDPT is formed with only four unknowns and we can introduce it at any material point of the EG plate as follows:

$$\begin{aligned}
u(x, y, z) &= u_0(x, y) - z \frac{\partial w_0(x, y)}{\partial x} + k_1 f(z) \int \theta(x, y) dx \\
v(x, y, z) &= v_0(x, y) - z \frac{\partial w_0(x, y)}{\partial y} + k_2 f(z) \int \theta(x, y) dy \\
w(x, y, z) &= w_0(x, y)
\end{aligned} \tag{III.4}$$

We should mention that $\theta(x, y)$ is a mathematical term which helps us to get the rotations value of the normal to the mid-plate according to the x and y axes. k_1 and k_2 are the coefficients related to the plate geometry under consideration.

The integrals used in the aforementioned relations shall be resolved by the Navier-type method which leads to the following introduced expression as follows:

$$\int \theta(x, y) dx = A' \frac{\partial \theta(x, y)}{\partial x}, \quad \int \theta(x, y) dy = B' \frac{\partial \theta(x, y)}{\partial y} \tag{III.5}$$

The displacement field at any point of the plate can be rewritten as below

$$\begin{aligned}
u(x, y, z) &= u_0(x, y) - z \frac{\partial w_0(x, y)}{\partial x} + k_1 A' f(z) \frac{\partial \theta(x, y)}{\partial x} \\
v(x, y, z) &= v_0(x, y) - z \frac{\partial w_0(x, y)}{\partial y} + k_2 B' f(z) \frac{\partial \theta(x, y)}{\partial y} \\
w(x, y, z) &= w_0(x, y)
\end{aligned} \tag{III.6}$$

In which the coefficients A' , B' , k_1 and k_2 can be defined by

$$A' = -\frac{1}{\alpha^2}, \quad B' = -\frac{1}{\beta^2}, \quad k_1 = \alpha^2, \quad k_2 = \beta^2 \quad (\text{III.7})$$

Where the parameters α and β are defined as follows:

$$\alpha = \frac{m\pi}{a}, \quad \beta = \frac{n\pi}{b} \quad (\text{III.8})$$

The mentioned displacement field in Equation III.4 deals only with four unknowns u_0, v_0, w_0 and θ . When the shape function $f(z)$ is given according to the following form:

$$f(z) = \frac{7}{4}z - \frac{7z^3}{3h^2} \quad (\text{III.9})$$

We should note that the aim of using the shear polynomial function in the proposed theory is to meeting zero stresses on both of the top and bottom surfaces of the EG plate.

The differential of the shear function is obtained as follows:

$$g(z) = \frac{df(z)}{dz} = \frac{7}{4} - \frac{7z^2}{h^2} \quad (\text{III.10})$$

The nonzero strains related to the displacement field in Equation III.4 are as follows:

$$\begin{Bmatrix} \varepsilon_x \\ \varepsilon_y \\ \gamma_{xy} \end{Bmatrix} = \begin{Bmatrix} \varepsilon_x^0 \\ \varepsilon_y^0 \\ \varepsilon_{xy}^0 \end{Bmatrix} + z \begin{Bmatrix} k_x^b \\ k_y^b \\ k_{xy}^b \end{Bmatrix} + f(z) \begin{Bmatrix} k_x^s \\ k_y^s \\ k_{xy}^s \end{Bmatrix}, \quad \begin{Bmatrix} \gamma_{yz}^s \\ \gamma_{xz}^s \end{Bmatrix} = g(z) \begin{Bmatrix} \gamma_{yz}^0 \\ \gamma_{xz}^0 \end{Bmatrix} \quad (\text{III.11})$$

Where:

$$\begin{Bmatrix} \varepsilon_x^0 \\ \varepsilon_y^0 \\ \varepsilon_{xy}^0 \end{Bmatrix} = \begin{Bmatrix} \frac{\partial u_0}{\partial x} \\ \frac{\partial v_0}{\partial y} \\ \frac{\partial u_0}{\partial y} + \frac{\partial v_0}{\partial x} \end{Bmatrix}, \quad \begin{Bmatrix} k_x^b \\ k_y^b \\ k_{xy}^b \end{Bmatrix} = \begin{Bmatrix} -\frac{\partial^2 w_0}{\partial x^2} \\ -\frac{\partial^2 w_0}{\partial y^2} \\ -2\frac{\partial^2 w_0}{\partial x \partial y} \end{Bmatrix}, \quad \begin{Bmatrix} k_x^s \\ k_y^s \\ k_{xy}^s \end{Bmatrix} = \begin{Bmatrix} k_1 A' \frac{\partial^2 \theta}{\partial x^2} \\ k_2 B' \frac{\partial^2 \theta}{\partial y^2} \\ (k_1 A' + k_2 B') \frac{\partial^2 \theta}{\partial x \partial y} \end{Bmatrix}, \quad (\text{III.12})$$

$$\begin{Bmatrix} \gamma_{yz}^0 \\ \gamma_{xz}^0 \end{Bmatrix} = \begin{Bmatrix} k_2 B' \frac{\partial \theta}{\partial y} \\ k_1 A' \frac{\partial \theta}{\partial x} \end{Bmatrix}$$

Regarding to the stress-strain relationships accounting for transversal shear deformation in the EG plates coordinates, can be obtained in matrix forms as follows:

$$\begin{Bmatrix} \sigma_x \\ \sigma_y \\ \tau_{xy} \end{Bmatrix} = \begin{bmatrix} Q_{11} & Q_{12} & 0 \\ Q_{12} & Q_{22} & 0 \\ 0 & 0 & Q_{66} \end{bmatrix} \begin{Bmatrix} \varepsilon_x \\ \varepsilon_y \\ \gamma_{xy} \end{Bmatrix}, \quad \begin{Bmatrix} \tau_{yz} \\ \tau_{xz} \end{Bmatrix} = \begin{bmatrix} Q_{44} & 0 \\ 0 & Q_{55} \end{bmatrix} \begin{Bmatrix} \gamma_{yz}^s \\ \gamma_{xz}^s \end{Bmatrix} \quad (\text{III.13})$$

Where $\{\sigma_x, \sigma_y, \tau_{xy}, \tau_{yz}, \tau_{xz}\}^{Tr}$, and $\{\varepsilon_x, \varepsilon_y, \gamma_{xy}, \gamma_{yz}, \gamma_{xz}\}^{Tr}$ are the stresses and the strains vectors respectively referenced to the plate Coordinate system. Despite, the two-dimensional elastic constants Q_{ij} are introduced in engineering constants terms as follows:

$$Q_{11} = Q_{22} = \frac{E(z)}{(1-\nu^2)}, \quad Q_{12} = \nu Q_{11}, \quad Q_{44} = Q_{55} = Q_{66} = \frac{E(z)}{2(1+\nu)} \quad (\text{III.14})$$

III.3. Governing differential equations

Considering the proposed higher-order plate theory in the case of the inhomogeneous EG plate, we should mention that both of governing differential equations and boundary conditions are derived by using the principle of virtual work. This principle can be expressed in the following analytical form:

$$\int_{-h/2}^{h/2} \int_A (\sigma_x \delta \varepsilon_x + \sigma_y \delta \varepsilon_y + \sigma_z \delta \varepsilon_z + \tau_{xy} \delta \gamma_{xy} + \tau_{yz} \delta \gamma_{yz} + \tau_{xz} \delta \gamma_{xz}) dA dz - \int_A q \delta w dA = 0 \quad (\text{III.15})$$

Where δ denotes the variational operator and q mentions to the transverse distributed load applied on the top surface of the plate. The principle of virtual work can be obtained by substituting the expressions for virtual strains given in Equation III.11 with those in Equation III.15, so we get the following expression:

$$\begin{aligned} & \int_A [N_x \delta \varepsilon_x^0 + N_y \delta \varepsilon_y^0 + N_{xy} \delta \gamma_{xy}^0 + M_x^b \delta \varepsilon_x^b + M_y^b \delta \varepsilon_y^b + M_{xy}^b \delta \gamma_{xy}^b + M_x^s \delta \varepsilon_x^s \\ & + M_y^s \delta \varepsilon_y^s + M_{xy}^s \delta \gamma_{xy}^s + S_{yz}^s \delta \gamma_{yz}^0 + S_{xz}^s \delta \gamma_{xz}^0 - q \delta w] dA = 0 \end{aligned} \quad (\text{III.16})$$

Where N, M^b, M^s , and S^s are the stress resultants defined by the following mentioned integrations over the thickness of the plate:

$$\begin{Bmatrix} N_x & N_y & N_{xy} \\ M_x^b & M_y^b & M_{xy}^b \\ M_x^s & M_y^s & M_{xy}^s \end{Bmatrix} = \int_{-h/2}^{h/2} (\sigma_x, \sigma_y, \tau_{xy}) \begin{Bmatrix} 1 \\ z \\ f(z) \end{Bmatrix} dz, \quad (\text{III.17})$$

$$(S_{xz}^s, S_{yz}^s) = \int_{-h/2}^{h/2} (\tau_{xz}, \tau_{yz}) g(z) dz$$

The stress resultants of the proposed theory can be obtained in terms of strains according to the following matrix form by replacing Equation III.11 into Equation III.13 which contains stress–strain relations in addition to the subsequent results given in Equation III.17:

$$\begin{Bmatrix} N_x \\ N_y \\ N_{xy} \\ M_x^b \\ M_y^b \\ M_{xy}^b \\ M_x^s \\ M_y^s \\ M_{xy}^s \end{Bmatrix} = \begin{bmatrix} A_{11} & A_{12} & 0 & B_{11} & B_{12} & 0 & E_{11} & E_{12} & 0 \\ A_{12} & A_{22} & 0 & B_{12} & B_{22} & 0 & E_{12} & E_{22} & 0 \\ 0 & 0 & A_{66} & 0 & 0 & B_{66} & 0 & 0 & E_{66} \\ B_{11} & B_{12} & 0 & D_{11} & D_{12} & 0 & F_{11} & F_{12} & 0 \\ B_{12} & B_{22} & 0 & D_{12} & D_{22} & 0 & F_{12} & F_{22} & 0 \\ 0 & 0 & B_{66} & 0 & 0 & D_{66} & 0 & 0 & F_{66} \\ E_{11} & E_{12} & 0 & F_{11} & F_{12} & 0 & H_{11} & H_{12} & 0 \\ E_{12} & E_{22} & 0 & F_{12} & F_{22} & 0 & H_{12} & H_{22} & 0 \\ 0 & 0 & E_{66} & 0 & 0 & F_{66} & 0 & 0 & H_{66} \end{bmatrix} \begin{Bmatrix} \varepsilon_x^0 \\ \varepsilon_y^0 \\ \gamma_{xy}^0 \\ \varepsilon_x^b \\ \varepsilon_y^b \\ \gamma_{xy}^b \\ \varepsilon_x^s \\ \varepsilon_y^s \\ \gamma_{xy}^s \end{Bmatrix} \quad (\text{III.18a})$$

$$\begin{Bmatrix} S_{yz}^s \\ S_{xz}^s \end{Bmatrix} = \begin{bmatrix} A_{44}^s & 0 \\ 0 & A_{55}^s \end{bmatrix} \begin{Bmatrix} \gamma_{yz}^0 \\ \gamma_{xz}^0 \end{Bmatrix} \quad (\text{III.18b})$$

Where A_{ij} , B_{ij} , D_{ij} , E_{ij} , F_{ij} , H_{ij} , and A_{ij}^s are the plate stiffness coefficients, represented according to the following form:

$$(A_{ij}, B_{ij}, D_{ij}, B_{ij}^s, D_{ij}^s, H_{ij}^s, A_{ij}^s) = \int_{-h/2}^{h/2} Q_{ij}(1, z, z^2, f(z), z f(z), f^2(z), g^2(z)) dz \quad (\text{III.19})$$

The substituting strains and stresses expressions from both of Equations III.12 and III.13 into Equation III.16 and integrating by parts and setting the coefficients of δu_0 , δv_0 , δw_0 and $\delta \theta$ equal to zero, leads to the obtained governing differential equations in stress resultants terms as follows:

$$\begin{aligned} \delta u_0 : \frac{\partial N_x}{\partial x} + \frac{\partial N_{xy}}{\partial y} &= 0 \\ \delta v_0 : \frac{\partial N_{xy}}{\partial x} + \frac{\partial N_y}{\partial y} &= 0 \\ \delta w_0 : \frac{\partial^2 M_x^b}{\partial x^2} + 2 \frac{\partial^2 M_{xy}^b}{\partial x \partial y} + \frac{\partial^2 M_y^b}{\partial y^2} + q &= 0 \\ \delta \theta : -k_1 A' \frac{\partial^2 M_x^s}{\partial x^2} - k_2 B' \frac{\partial^2 M_y^s}{\partial y^2} - (k_1 A' + k_2 B') \frac{\partial^2 M_{xy}^s}{\partial x \partial y} + k_1 A' \frac{\partial S_{xz}^s}{\partial x} + k_2 B' \frac{\partial S_{yz}^s}{\partial y} &= 0 \end{aligned} \quad (\text{III.20})$$

The governing differential equations (Equation III.20) can be reformed in displacement variables terms (u_0, v_0, w_0, θ) thanks to both of the present approach and using Equations III.12 and III.18 as illustrated in the following expressions:

$$\begin{aligned} \delta u_0 : & A_{11} \frac{\partial^2 u_0}{\partial x^2} + A_{66} \frac{\partial^2 u_0}{\partial y^2} + (A_{12} + A_{66}) \frac{\partial^2 v_0}{\partial x \partial y} - B_{11} \frac{\partial^3 w_0}{\partial x^3} - (B_{12} + 2B_{66}) \frac{\partial^3 w_0}{\partial x \partial y^2} \\ & + k_1 A' \frac{\partial^3 \theta}{\partial x^3} E_{11} + k_2 B' E_{12} \frac{\partial^3 \theta}{\partial x \partial y^2} + (k_1 A' + k_2 B') E_{66} \frac{\partial^3 \theta}{\partial x \partial y^2} = 0 \end{aligned} \quad (III.21a)$$

$$\begin{aligned} \delta v_0 : & (A_{12} + A_{66}) \frac{\partial^2 u_0}{\partial x \partial y} + A_{22} \frac{\partial^2 v_0}{\partial y^2} + A_{66} \frac{\partial^2 v_0}{\partial x^2} - (B_{12} + 2B_{66}) \frac{\partial^3 w_0}{\partial x^2 \partial y} - B_{22} \frac{\partial^3 w_0}{\partial y^3} \\ & + k_1 A' E_{12} \frac{\partial^3 \theta}{\partial x^2 \partial y} + k_2 B' E_{22} \frac{\partial^3 \theta}{\partial y^3} + (k_1 A' + k_2 B') E_{66} \frac{\partial^3 \theta}{\partial x^2 \partial y} = 0 \end{aligned} \quad (III.21b)$$

$$\begin{aligned} \delta w_0 : & B_{11} \frac{\partial^3 u_0}{\partial x^3} + (B_{12} + 2B_{66}) \frac{\partial^3 u_0}{\partial x \partial y^2} + F_{12} (k_1 A' + k_2 B') \frac{\partial^4 \theta}{\partial y^2 \partial x^2} + B_{22} \frac{\partial^3 v_0}{\partial y^3} \\ & + (B_{12} + 2B_{66}) \frac{\partial^3 v_0}{\partial x^2 \partial y} - D_{11} \frac{\partial^4 w_0}{\partial x^4} - D_{22} \frac{\partial^4 w_0}{\partial y^4} - 2(D_{12} + 2D_{66}) \frac{\partial^4 w_0}{\partial x^2 \partial y^2} \\ & + (k_1 A' F_{11}) \frac{\partial^4 \theta}{\partial x^4} + 2(k_1 A' + k_2 B') F_{66} \frac{\partial^4 \theta}{\partial x^2 \partial y^2} + (k_2 B' F_{22}) \frac{\partial^4 \theta}{\partial y^4} + q = 0 \end{aligned} \quad (III.21c)$$

$$\begin{aligned} \delta \theta : & -k_1 A' \left(\left(\frac{\partial^3}{\partial x^3} u_0(x, y) \right) E_{11} - \left(\frac{\partial^4}{\partial x^4} w_0(x, y) \right) F_{11} + k_1 A' \left(\frac{\partial^4}{\partial x^4} \theta(x, y) \right) H_{11} \right. \\ & \left. + \left(\frac{\partial^3}{\partial y \partial x^2} v_0(x, y) \right) E_{12} - \left(\frac{\partial^4}{\partial y^2 \partial x^2} w_0(x, y) \right) F_{12} + k_2 B' \left(\frac{\partial^4}{\partial y^2 \partial x^2} \theta(x, y) \right) H_{12} \right) \\ & - k_2 B' \left(\left(\frac{\partial^3}{\partial y^2 \partial x} u_0(x, y) \right) E_{12} - \left(\frac{\partial^4}{\partial y^2 \partial x^2} w_0(x, y) \right) F_{12} + k_1 A' \left(\frac{\partial^4}{\partial y^2 \partial x^2} \theta(x, y) \right) H_{12} \right. \\ & \left. + \left(\frac{\partial^3}{\partial y^3} v_0(x, y) \right) E_{22} - \left(\frac{\partial^4}{\partial y^4} w_0(x, y) \right) F_{22} + k_2 B' \left(\frac{\partial^4}{\partial y^4} \theta(x, y) \right) H_{22} \right) \\ & - (k_1 A' + k_2 B') \left(\left(\frac{\partial^3}{\partial y^2 \partial x} u_0(x, y) \right) E_{66} - 2 \left(\frac{\partial^4}{\partial y^2 \partial x^2} w_0(x, y) \right) F_{66} \right. \\ & \left. + k_1 A' \left(\frac{\partial^4}{\partial y^2 \partial x^2} \theta(x, y) \right) H_{66} + \left(\frac{\partial^3}{\partial y \partial x^2} v_0(x, y) \right) E_{66} + k_2 B' \left(\frac{\partial^4}{\partial y^2 \partial x^2} \theta(x, y) \right) H_{66} \right) \\ & + (k_1 A')^2 \left(\frac{\partial^2}{\partial x^2} \theta(x, y) \right) A_{55}^s + (k_2 B')^2 \left(\frac{\partial^2}{\partial y^2} \theta(x, y) \right) A_{44}^s = 0 \end{aligned} \quad (III.21d)$$

III.4. Analytical solution for EG plates

According to the present PSDPT theory, the bending analysis of a simply supported exponentially graded plate is obtained by using Navier solution technique. The boundary conditions along the edges of the simply supported EG plate can be expressed as

On edges ($x = 0, a$)

$$v_0 = w_0 = N_x = M_x^b = M_x^s = \theta = 0 \quad (III.22a)$$

On edges ($y = 0, b$)

$$u_0 = w_0 = N_y = M_y^b = M_y^s = \theta = 0 \quad (III.22b)$$

In this study, We should mention that the analytical solutions of Eq. (III.21) for simply supported thick EG plates under transverse mechanical loading can be obtained, by considering the Navier's solution technique, the following expressions of four-unknown variables are represented in the double trigonometric series, which satisfy the governing equations and its boundary conditions exactly:

$$\begin{Bmatrix} u_0 \\ v_0 \\ w_0 \\ \theta \end{Bmatrix} = \sum_{m=1}^{\infty} \sum_{n=1}^{\infty} \begin{Bmatrix} U_{mn} \cos(\alpha x) \sin(\beta y) \\ V_{mn} \sin(\alpha x) \cos(\beta y) \\ W_{mn} \sin(\alpha x) \sin(\beta y) \\ \Theta_{mn} \sin(\alpha x) \sin(\beta y) \end{Bmatrix} \quad (III.23)$$

Where U_{mn} , V_{mn} , W_{mn} , and Θ_{mn} are unknown coefficients. The parameters α , and β are already defined in aforementioned Equation III.8. However, $q(x, y)$ represents the transverse load which is acting on the top surface of the plate and is also expanded in the double-Fourier sine series as illustrated in the next form:

$$q(x, y) = \sum_{m=1}^{\infty} \sum_{n=1}^{\infty} Q_{mn} \sin(\alpha x) \cos(\beta y) \quad (III.24)$$

We should note that in the case of sinusoidal distributed load $Q_{mn} = q_0$ and $m = n = 1$ in which q_0 denotes the maximum intensity of the external load along the z direction. We can introduce the analytical solutions of EG plates in matrix form by the substituting the Equations III.23 and III.24 solution into the governing equations given in Equation III.21:

$$[K]\{U\} = \{F\} \quad (III.25)$$

Either in expanded form:

$$\begin{bmatrix} K_{11} & K_{12} & K_{13} & K_{14} \\ K_{21} & K_{22} & K_{23} & K_{24} \\ K_{31} & K_{32} & K_{33} & K_{34} \\ K_{41} & K_{42} & K_{43} & K_{44} \end{bmatrix} \begin{Bmatrix} U_{mn} \\ V_{mn} \\ W_{mn} \\ \Theta_{mn} \end{Bmatrix} = \begin{Bmatrix} 0 \\ 0 \\ Q_{mn} \\ 0 \end{Bmatrix} \quad (\text{III.26})$$

Where the elements of stiffness matrix $[K_{ij}]$ are introduced as follows:

$$\begin{aligned} k_{11} &= \alpha^2 A_{11} + \beta^2 A_{66}, \\ k_{12} &= \alpha\beta A_{12} + \alpha\beta A_{66}, \\ k_{13} &= -\alpha^3 B_{11} - \alpha\beta^2 B_{12} - 2\alpha\beta^2 B_{66}, \\ k_{14} &= -k_1 A' \alpha^3 E_{11} - k_2 B' \alpha\beta^2 E_{12} + (k_1 A' + k_2 B') \alpha\beta^2 E_{66}, \\ k_{21} &= \alpha\beta^2 A_{12} + \alpha\beta A_{66}, \\ k_{22} &= \beta^2 A_{22} + \alpha^2 A_{66} \\ k_{23} &= -\beta^3 B_{22} - \alpha^2 \beta B_{12} - 2\alpha^2 \beta B_{66}, \\ k_{24} &= -k_1 A' \alpha^2 \beta E_{12} - k_2 B' \beta^3 E_{22} + (k_1 A' + k_2 B') \alpha^2 \beta E_{66}, \\ k_{31} &= -2\alpha\beta^2 B_{66} - \alpha\beta^2 B_{12} - \alpha^3 B_{11} \\ k_{32} &= -2\alpha^2 \beta B_{66} - \beta^3 B_{22} - \alpha^2 \beta B_{12} \\ k_{33} &= \alpha^4 D_{11} + 2\alpha^2 \beta^2 D_{12} + \beta^4 D_{22} + 4\alpha^2 \beta^2 D_{66}, \\ k_{34} &= k_1 A' (\alpha^4 F_{11} + \beta^2 F_{12}) + k_2 B' \beta^2 (\alpha^2 F_{12} + \beta^2 F_{22}) - 2(k_1 A' + k_2 B') \alpha^2 \beta^2 F_{66}, \\ k_{41} &= k_1 A' \alpha^3 E_{11} + (k_1 A' + k_2 B') \alpha\beta^2 E_{66} + k_2 B' \alpha\beta^2 E_{12} \\ k_{42} &= k_1 A' \alpha^2 \beta E_{12} + (k_1 A' + k_2 B') \alpha^2 \beta E_{66} + k_2 B' \beta^3 E_{22} \\ k_{43} &= k_1 A' (-\alpha^2 \beta^2 F_{12} - \alpha^4 F_{11}) + k_2 B' (-\beta^4 F_{22} - \alpha^2 \beta^2 F_{12}) - 2(k_1 A' + k_2 B') \alpha^2 \beta^2 F_{66} \\ k_{44} &= -(k_1 A' + k_2 B')^2 \alpha^2 \beta^2 H_{66} + k_1 A' (k_1 A' \alpha^4 H_{11} + k_2 \beta' \alpha^2 \beta^2 H_{12}) \\ &\quad + k_2 B' (k_1 A' \alpha^2 \beta^2 H_{12} + k_2 B' \beta^4 H_{22}) + (k_2 B')^2 \beta^4 A_{44}^s + (k_1 A')^2 \alpha^2 A_{55}^s, \end{aligned} \quad (\text{III.27})$$

III.5. Conclusion

In our work we aim to study the static response of thick exponentially graded (EG) plates, for that reason it is necessary to analyze the bending of considered plates which is one of the important parts that enable us to investigate height accuracy with better stability of the structures.

In this chapter we have presented the new displacement field of the present high-order shear deformation theory which takes into consideration the transverse shear effect of FGM plates, which their material properties vary through the thickness according to an exponential function (E-FGM). The number of unknowns in this refined theory is only four compared to the other conventional refined shear deformation theories of high-order, and thanks to the

development of theoretical formulations based on the laws of static behavior we have arrived at an analytical model of the bending of the exponentially graded plates without requiring shear correction factors. The equilibrium differential equations are achieved through the application of virtual work principle. Solutions are obtained using the Navier-type procedure, and the analytical solutions for displacements and stresses are found by solving the matrix form of the resulting system.

■ *Chapter IV*

Numerical results and discussion

Chapter IV

Numerical results and discussion

IV.1. Introduction

The interest of this chapter is to present the numerical results of simply supported exponentially graded plates (EGPs) using a new parabolic shear deformation plate theory (PSDPT) that we developed in the previous chapter. It is assumed that the material properties of the FG plate vary in the thickness direction according to the exponential model depending on the volume fraction of the constituents. In this theory the stretching effect through the thickness of the plate is negligible and number of unknowns in this new theory is four, unlike other high-order theories. In the following, numerical results are presented for various aspect ratios (b/a), side-to-thickness ratios (a/h) and different values of the power-law exponent p

These numerical results are compared with:

- The well-known trigonometric shear deformation plate theory “TSDPT” which involves sinus function primary developed by the collaboration of Levy and Stein, and used by Touratier and became lately applicable to both of the power-law distribution “P-FGM” and exponential-law distribution “E-FGM” by Zenkour on the basis of the quasi-3D model;
- The results provided by Zenkour based on the quasi-3D higher-order shear deformation plate theory “HSDPT”;
- A recently 2D higher-order shear deformation plate theory “HSDPT” developed by Mantari and Guedes Soares [59], which were successfully appropriate for the E-FGM by the collaboration of Mantari and Guedes Soares;
- A 3D exact solution.

IV.2. Numerical results and discussion

In this study, the functionally grade material plates made of a mixture between two distributed isotropic constituents with a continuous gradient through the thickness direction of a rectangular plate are provided and used to examine the static bending behavior of simply supported EG plates subjected to sinusoidal distributed load, by using the simple and accurate higher-order parabolic shear deformation theory.

The considered plate is made of a combination of both aluminum as metal (bottom surface) and alumina as ceramic (top surface). We should mention that the effective material properties, such as Young's modulus vary exponentially through the thickness of the plate according to the volume fractions of the constituents via the exponential function as reported by Mantari and Guedes Soares [1].

The non-dimensional displacements and stresses are presented and compared with the corresponding results of various higher-order shear deformation theories available in literature and the exact elasticity solution given by Zenkour [13] wherever applicable. The material properties of the exponentially graded (EG) square and rectangular plate used for calculating the numerical results are:

$$E_m = 70 \text{ GPa}, \quad \nu_m = \nu_c = \nu = 0.3 \quad (\text{IV.1})$$

In the present study, the results obtained for displacements, stresses components are reported with the following generalized non-dimensional forms:

$$\begin{aligned} \bar{u}\left(0, \frac{b}{2}, z\right) &= \frac{10h^3 E_b}{qa^4} u, & \bar{v}\left(\frac{a}{2}, 0, z\right) &= \frac{10h^3 E_b}{qa^4} v, \\ \bar{w}\left(\frac{a}{2}, \frac{b}{2}, z\right) &= \frac{10h^3 E_b}{qa^4} w, & \bar{\sigma}_x\left(\frac{a}{2}, \frac{b}{2}, z\right) &= \frac{h^2}{qa^2} \sigma_x, \\ \bar{\sigma}_y\left(\frac{a}{2}, \frac{b}{2}, z\right) &= \frac{h^2}{qa^2} \sigma_y, & \bar{\tau}_{xy}(0, 0, z) &= \frac{h^2}{qa^2} \tau_{xy}, \\ \bar{\tau}_{xz}\left(0, \frac{b}{2}, z\right) &= \frac{h}{qa} \tau_{xz}, & \bar{\tau}_{yz}\left(\frac{a}{2}, 0, z\right) &= \frac{h}{qa} \tau_{yz} \end{aligned} \quad (\text{IV.2})$$

IV.2.1 Validation study

In this theoretical study, displacements and stresses calculated according to Equation (IV.2) in non-dimensional form are presented and compared with the results of various shear deformation theories to validate the precision and accuracy of the present four-variable unknown plate theory. Tables IV.1 to IV.7 show the comparison of the transverse displacements and stresses for simply supported exponentially graded square and rectangular plates subjected to sinusoidal distributed load for various values of aspect ratio ($b/a = 1, 2, 3, 4, 5, 6$), side-to-thickness ratio ($a/h = 2, 4, 10$), and power-law exponent p . The material properties of EG plates used in this study are given in Equation (IV.1). In order to assure the accuracy of the proposed theory, the numerical results obtained for this example are compared

with the results predicted by Mantari and Guedes Soares [1] using a 2D higher-order shear deformation plate theory (HSDPT), the analytical solutions reported by Zenkour [13] based on the quasi-3D trigonometric shear deformation plate theory (TSDPT), the quasi-3D higher-order shear deformation plate theory (HSDPT) and 3-D elasticity solution also given by Zenkour [13].

Table IV.1: Non-dimensional transverse displacement $\bar{w}(a/2, b/2, 0)$ for various power-law exponent of EG square and rectangular plates, $a/h = 2$.

b/a	Theory	Model	p					
			0.1	0.3	0.5	0.7	1.0	1.5
5	Present	PSDPT	1.70241	1.53968	1.39185	1.25760	1.07913	0.83401
	Ref. [1] ^(*)	HSDPT	1.70246	1.53972	1.39188	1.25762	1.07981	0.83401
	Zenkour [13]	TSDPT	1.59825	1.44493	1.30522	1.17804	1.00856	0.77540
	Zenkour [13]	HSDPT	1.51991	1.37444	1.24214	1.12188	0.96184	0.74184
	Zenkour [13]	Exact	1.60646	1.46007	1.32607	1.20349	1.03907	0.81024
4	Present	PSDPT	1.64579	1.48845	1.34550	1.21567	1.04306	0.80596
	Ref. [1] ^(*)	HSDPT	1.64584	1.48849	1.34553	1.21569	1.04374	0.80596
	Zenkour [13]	TSDPT	1.54348	1.39541	1.26048	1.13764	0.97395	0.74874
	Zenkour [13]	HSDPT	1.47089	1.33009	1.20201	1.08559	0.93065	0.71762
	Zenkour [13]	Exact	1.55146	1.41013	1.28074	1.16235	1.00352	0.78241
3	Present	PSDPT	1.53399	1.38730	1.25399	1.13289	0.97185	0.75060
	Ref. [1] ^(*)	HSDPT	1.53405	1.38735	1.25402	1.13291	0.97254	0.75060
	Zenkour [13]	TSDPT	1.43542	1.29771	1.17221	1.05795	0.90567	0.69615
	Zenkour [13]	HSDPT	1.37394	1.24238	1.12269	1.01386	0.86898	0.66977
	Zenkour [13]	Exact	1.44295	1.31160	1.19129	1.08117	0.93337	0.72750
2	Present	PSDPT	1.27754	1.15528	1.04410	0.94305	0.80859	0.62376
	Ref. [1] ^(*)	HSDPT	1.2776	1.15533	1.04413	0.94307	0.80929	0.62377
	Zenkour [13]	TSDPT	1.18798	1.07399	0.97009	0.87548	0.74936	0.57578
	Zenkour [13]	HSDPT	1.15080	1.04052	0.94012	0.84878	0.72712	0.55975
	Zenkour [13]	Exact	1.19445	1.08593	0.98640	0.89520	0.77266	0.60174
1	Present	PSDPT	0.63619	0.57512	0.51943	0.46871	0.40106	0.30788
	Ref. [1] ^(*)	HSDPT	0.63625	0.57517	0.51948	0.46874	0.40178	0.30791
	Zenkour [13]	TSDPT	0.57308	0.51806	0.46788	0.42216	0.36117	0.27712
	Zenkour [13]	HSDPT	0.58586	0.52955	0.47814	0.43127	0.36871	0.28246
	Zenkour [13]	Exact	0.57693	0.52473	0.47664	0.43240	0.37269	0.28904

^(*) Results taken from reference of Mantari and Guedes Soares [1]

Table IV.2: Non-dimensional transverse displacement $\bar{w}(a/2, b/2, 0)$ for various power-law exponent of EG square and rectangular plates, $a/h = 4$.

b/a	Theory	Model	p					
			0.1	0.3	0.5	0.7	1.0	1.5
5	Present	PSDPT	1.16627	1.05555	0.95557	0.86525	0.74579	0.58254
	Ref. [1] ^(*)	HSDPT	1.16628	1.05555	0.95557	0.86525	0.74578	0.58253
	Zenkour [13]	TSDPT	1.14140	1.03210	0.93268	0.84231	0.72212	0.55726
	Zenkour [13]	HSDPT	0.98508	0.89150	0.80694	0.73050	0.62935	0.49105
	Zenkour [13]	Exact	1.14589	1.03906	0.94236	0.85478	0.73859	0.57904
4	Present	PSDPT	1.12113	1.01468	0.91856	0.83172	0.71686	0.55988
	Ref. [1] ^(*)	HSDPT	1.12113	1.01469	0.91856	0.83172	0.71685	0.55987
	Zenkour [13]	TSDPT	1.09682	0.99180	0.89625	0.80941	0.69390	0.53546
	Zenkour [13]	HSDPT	0.94753	0.85750	0.77615	0.70262	0.60529	0.47222
	Zenkour [13]	Exact	1.10115	0.99852	0.90560	0.82145	0.70979	0.55643
3	Present	PSDPT	1.03254	0.93449	0.84594	0.76593	0.66008	0.51542
	Ref. [1] ^(*)	HSDPT	1.03254	0.9345	0.84594	0.76593	0.66008	0.51541
	Zenkour [13]	TSDPT	1.00938	0.91272	0.82479	0.74486	0.63854	0.49270
	Zenkour [13]	HSDPT	0.87379	0.79076	0.71571	0.64787	0.55806	0.43525
	Zenkour [13]	Exact	1.01338	0.91899	0.83350	0.75606	0.65329	0.51209
2	Present	PSDPT	0.83245	0.75337	0.68192	0.61734	0.53188	0.41504
	Ref. [1] ^(*)	HSDPT	0.83246	0.75338	0.68192	0.61734	0.53188	0.41503
	Zenkour [13]	TSDPT	0.81202	0.73425	0.66350	0.59917	0.51361	0.39620
	Zenkour [13]	HSDPT	0.70700	0.63979	0.57901	0.52405	0.45126	0.35169
	Zenkour [13]	Exact	0.81529	0.73946	0.67075	0.60846	0.52574	0.41200
1	Present	PSDPT	0.36016	0.32588	0.29485	0.26676	0.22952	0.17854
	Ref. [1] ^(*)	HSDPT	0.36017	0.32589	0.29485	0.26676	0.22952	0.17854
	Zenkour [13]	TSDPT	0.34749	0.31419	0.28388	0.25631	0.21961	0.16922
	Zenkour [13]	HSDPT	0.31111	0.28146	0.25461	0.23027	0.19800	0.15377
	Zenkour [13]	Exact	0.34900	0.31677	0.28747	0.26083	0.22534	0.18054

^(*) Results Taken from reference of Mantari and Guedes Soares [1]

According to Tables IV.1, IV.2, and IV.3, it can be observed that the numerical results of transverse displacements obtained by using the present parabolic shear deformation plate theory (PSDPT) are in excellent agreement with the HSDPT of Mantari and Guedes Soares [1] for all aspect ratio and different values of power-law exponent p . However, a slight difference was found between 2D theory models (PSDPT and HSDPT) which do not include the thickness stretching effect and high-order quasi-3D theories due to the neglect of transverse normal deformation. Furthermore, the results obtained by Zenkour [13] based on quasi-3D models in which the stretching effect is taken into account are much closer to the exact

elasticity solutions for all aspect ratio and power-law exponent values ranging from very thick ($a/h = 2$) to moderately thick ($a/h = 10$) exponentially graded plates.

Table IV.3: Non-dimensional transverse displacement $\bar{w}(a/2, b/2, 0)$ for various power-law exponent of EG square and rectangular plates, $a/h = 10$.

b/a	Theory	Model	p						
			0.1	0.3	0.5	0.7	1.0	1.5	2
6	Present	PSDPT	1.03883	0.94052	0.85201	0.77225	0.66701	0.52356	0.41154
	Ref. [1] ^(*)	HSDPT	1.03883	0.94053	0.85202	0.77225	0.66702	0.52355	0.41154
	Zenkour [13]	TSDPT	1.03208	0.93335	0.84360	0.76209	0.65379	0.50542	0.39005
5	Present	PSDPT	1.01489	0.91885	0.83238	0.75446	0.65164	0.51148	0.40205
	Ref. [1] ^(*)	HSDPT	1.01490	0.91886	0.83238	0.75446	0.65164	0.51148	0.40204
	Zenkour [13]	TSDPT	1.00827	0.91181	0.82413	0.74451	0.63870	0.49376	0.38104
4	Present	PSDPT	0.97296	0.88089	0.79799	0.72328	0.62470	0.49033	0.38541
	Ref. [1] ^(*)	HSDPT	0.97297	0.88089	0.79799	0.72328	0.62471	0.49033	0.38540
	Zenkour [13]	TSDPT	0.96655	0.87408	0.79003	0.71370	0.61227	0.47332	0.36527
3	Present	PSDPT	0.89087	0.80657	0.73065	0.66224	0.57197	0.44892	0.35284
	Ref. [1] ^(*)	HSDPT	0.89088	0.80657	0.73066	0.66224	0.57198	0.44892	0.35283
	Zenkour [13]	TSDPT	0.88487	0.80022	0.72327	0.65338	0.56052	0.43331	0.33438
2	Present	PSDPT	0.70657	0.63970	0.57948	0.52521	0.45359	0.35595	0.27972
	Ref. [1] ^(*)	HSDPT	0.70657	0.63970	0.57948	0.52521	0.45359	0.35595	0.27972
	Zenkour [13]	TSDPT	0.70152	0.63441	0.57340	0.51799	0.44436	0.34349	0.26505
1	Present	PSDPT	0.28163	0.25496	0.23094	0.20928	0.18068	0.14168	0.11123
	Ref. [1] ^(*)	HSDPT	0.28164	0.25497	0.23094	0.20928	0.18069	0.14169	0.11123
	Zenkour [13]	TSDPT	0.27901	0.25231	0.22804	0.20600	0.17670	0.13655	0.10532

^(*) Results taken from reference of Mantari and Guedes Soares [1]

On the other hand, it may be noted that the results for the non-dimensional transverse displacements increase with the decrease of the exponent parameter p and the increase of the aspect ratio (b/a), it is clearly that this is due to the reduction in the plate stiffness. However, 2D theories that do not take into account the effect of thickness stretching tend to overestimate the results of \bar{w} across various proposed models, as they neglect transverse normal deformation.

Table IV.4: Non-dimensional in-plane normal stresses $\bar{\sigma}_{xx}(a/2, b/2, h/2)$ for various power-law exponent of EG square and rectangular plates, $a/h = 10$.

b/a	Theory	Model	p						
			0.1	0.3	0.5	0.7	1.0	1.5	2
6	Present	PSDPT	0.60288	0.64428	0.68826	0.73500	0.81072	0.95359	1.12040
	Ref. [1] ^(*)	HSDPT	0.60287	0.64427	0.68824	0.73499	0.81070	0.95356	1.12036
	Zenkour [13]	TSDPT	0.62706	0.67074	0.71703	0.76609	0.84523	0.99349	1.16507
5	Present	PSDPT	0.59097	0.63155	0.67466	0.72048	0.79470	0.93475	1.09827
	Ref. [1] ^(*)	HSDPT	0.59096	0.63154	0.67465	0.72047	0.79469	0.93473	1.09823
	Zenkour [13]	TSDPT	0.61489	0.65770	0.70307	0.75116	0.82874	0.97411	1.14238
4	Present	PSDPT	0.57004	0.60919	0.65077	0.69497	0.76657	0.90167	1.05940
	Ref. [1] ^(*)	HSDPT	0.57004	0.60918	0.65076	0.69496	0.76656	0.90165	1.05936
	Zenkour [13]	TSDPT	0.59350	0.63478	0.67854	0.72493	0.79977	0.94006	1.10251
3	Present	PSDPT	0.52884	0.56516	0.60374	0.64475	0.71118	0.83653	0.98287
	Ref. [1] ^(*)	HSDPT	0.52883	0.56515	0.60373	0.64474	0.71117	0.83650	0.98283
	Zenkour [13]	TSDPT	0.55135	0.58964	0.63023	0.67326	0.74272	0.87299	1.02396
2	Present	PSDPT	0.43498	0.46486	0.49661	0.53035	0.58501	0.68814	0.80854
	Ref. [1] ^(*)	HSDPT	0.43498	0.46486	0.49660	0.53034	0.58500	0.68812	0.80850
	Zenkour [13]	TSDPT	0.45521	0.48667	0.52004	0.55544	0.61263	0.72007	0.84487
1	Present	PSDPT	0.20621	0.22040	0.23547	0.25150	0.27745	0.32641	0.38355
	Ref. [1] ^(*)	HSDPT	0.20620	0.22039	0.23547	0.25149	0.27744	0.32640	0.38353
	Zenkour [13]	TSDPT	0.21957	0.23446	0.25028	0.26710	0.29439	0.34602	0.40655

^(*) Results taken from reference of Mantari and Guedes Soares [1]

Table IV.4 presented the comparison of non-dimensional in-plane normal stress $\bar{\sigma}_{xx}$ for simply supported square and rectangular exponentially graded plates subjected to sinusoidal distributed load for side-to-thickness ratio ($a/h = 10$) and various values of both aspect ratio (b/a) and power-law exponent p . Whereas Table IV.5 presents the comparison of non-dimensional in-plane normal stress $\bar{\sigma}_{yy}$ for side-to-thickness ratio ($a/h = 4$). This comparison also reveals that, the computed results are in excellent agreement with those calculated by other shear deformation theories as given by Mantari and Guedes Soares [1]. Furthermore, these results are compared with the exact elasticity solutions taking into account the stretching effect; therefore it is observable that they are in good agreement. From the results given in Tables IV.5, it can also be noted that the decrease of the values of power-law exponent p have a significant effect on the reduction of the in-plane normal stress $\bar{\sigma}_{yy}$.

Table IV.5: Non-dimensional in-plane normal stresses $\bar{\sigma}_{yy}(a/2, b/2, h/2)$ for various power-law exponent of EG square and rectangular plates, $a/h = 4$.

b/a	Theory	Model	p					
			0.1	0.3	0.5	0.7	1.0	1.5
5	Present	PSDPT	0.20368	0.21784	0.23288	0.24886	0.27473	0.32351
	Ref. [1] ^(*)	HSDPT	0.20366	0.21781	0.23285	0.24883	0.27470	0.32346
	Zenkour [13]	TSDPT	0.23912	0.25450	0.27097	0.28863	0.31764	0.37371
	Zenkour [13]	HSDPT	0.28261	0.30231	0.32323	0.34547	0.38148	0.44934
	Zenkour [13]	Exact	0.22060	0.23476	0.24984	0.26591	0.29199	0.34133
4	Present	PSDPT	0.20820	0.22267	0.23805	0.25439	0.28084	0.33071
	Ref. [1] ^(*)	HSDPT	0.20818	0.22264	0.23802	0.25435	0.28081	0.33066
	Zenkour [13]	TSDPT	0.24286	0.25858	0.27539	0.29342	0.32299	0.38004
	Zenkour [13]	HSDPT	0.28399	0.30379	0.32483	0.34719	0.38338	0.45159
	Zenkour [13]	Exact	0.22470	0.23918	0.25460	0.27103	0.29770	0.34816
3	Present	PSDPT	0.21621	0.23125	0.24723	0.26421	0.29170	0.34352
	Ref. [1] ^(*)	HSDPT	0.21619	0.23122	0.24720	0.26417	0.29166	0.34346
	Zenkour [13]	TSDPT	0.24931	0.26563	0.28307	0.30174	0.33230	0.39106
	Zenkour [13]	HSDPT	0.28588	0.30583	0.32702	0.34954	0.38601	0.45471
	Zenkour [13]	Exact	0.23188	0.24692	0.26295	0.28002	0.30775	0.36021
2	Present	PSDPT	0.22946	0.24545	0.26244	0.28049	0.30972	0.36480
	Ref. [1] ^(*)	HSDPT	0.22943	0.24542	0.26240	0.28045	0.30967	0.36473
	Zenkour [13]	TSDPT	0.25878	0.27609	0.29456	0.31428	0.34644	0.40788
	Zenkour [13]	HSDPT	0.28539	0.30534	0.32655	0.34908	0.38556	0.45428
	Zenkour [13]	Exact	0.24314	0.25913	0.27618	0.29434	0.32385	0.37968
1	Present	PSDPT	0.21640	0.23163	0.24780	0.26499	0.29280	0.34518
	Ref. [1] ^(*)	HSDPT	0.21636	0.23157	0.24774	0.26492	0.29273	0.34508
	Zenkour [13]	TSDPT	0.23457	0.25098	0.26842	0.28698	0.31706	0.37386
	Zenkour [13]	HSDPT	0.24080	0.25783	0.27593	0.29515	0.32627	0.38482
	Zenkour [13]	Exact	0.22472	0.23995	0.25621	0.27356	0.30177	0.35885

^(*) Results taken from reference of Mantari and Guedes Soares [1]

Tables IV.6 and IV.7 also show the comparison of in-plane normal stress $\bar{\sigma}_{yy}$ and transverse shear stress $\bar{\tau}_{xz}$, respectively for simply supported, moderately thick rectangular EG plates ($a/h = 10$). It is evident from the results that the present results are in an excellent agreement with the higher-order shear deformation plate theory reported by Mantari and Guedes Soares [1]. According to the analytical solutions given in Tables IV.6 and IV.7, it can be noticed that the increase of the values of power-law exponent p and the increase of aspect ratio (b/a) have a substantial effect on the decrease of the transverse shear stress $\bar{\tau}_{xz}$ for all the cases presented in this study.

Table IV.6: Non-dimensional in-plane normal stresses $\bar{\sigma}_{yy}(a/2, b/2, h/2)$ for various power-law exponent of EG square and rectangular plates, $a/h = 10$.

b/a	Theory	Model	p						
			0.1	0.3	0.5	0.7	1.0	1.5	2
6	Present	PSDPT	0.19598	0.20943	0.22373	0.23892	0.26354	0.30998	0.36420
	Ref. [1] ^(*)	HSDPT	0.19598	0.20943	0.22373	0.23892	0.26353	0.30997	0.36419
	Zenkour [13]	TSDPT	0.22228	0.23600	0.25070	0.26653	0.29261	0.34347	0.40538
5	Present	PSDPT	0.19854	0.21218	0.22666	0.24206	0.26699	0.31404	0.36898
	Ref. [1] ^(*)	HSDPT	0.19854	0.21218	0.22666	0.24205	0.26699	0.31404	0.36897
	Zenkour [13]	TSDPT	0.22454	0.23845	0.25337	0.26940	0.29582	0.34726	0.40976
4	Present	PSDPT	0.20283	0.21676	0.23156	0.24729	0.27276	0.32084	0.37696
	Ref. [1] ^(*)	HSDPT	0.20284	0.21676	0.23156	0.24729	0.27276	0.32083	0.37695
	Zenkour [13]	TSDPT	0.22827	0.24252	0.25778	0.27418	0.30115	0.35355	0.41703
3	Present	PSDPT	0.21040	0.22484	0.24020	0.25651	0.28294	0.33281	0.39103
	Ref. [1] ^(*)	HSDPT	0.21040	0.22484	0.24019	0.25651	0.28294	0.33280	0.39102
	Zenkour [13]	TSDPT	0.23470	0.24955	0.26543	0.28246	0.31041	0.36447	0.42964
2	Present	PSDPT	0.22255	0.23783	0.25408	0.27134	0.29931	0.35207	0.41367
	Ref. [1] ^(*)	HSDPT	0.22255	0.23783	0.25408	0.27134	0.29930	0.35206	0.41365
	Zenkour [13]	TSDPT	0.24411	0.25994	0.27684	0.29490	0.32441	0.38104	0.44861
1	Present	PSDPT	0.20621	0.22040	0.23547	0.25150	0.27745	0.32641	0.38355
	Ref. [1] ^(*)	HSDPT	0.20620	0.22039	0.23547	0.25149	0.27744	0.32640	0.38353
	Zenkour [13]	TSDPT	0.21957	0.23446	0.25028	0.26710	0.29439	0.34602	0.40655

^(*) Results taken from reference of Mantari and Guedes Soares [1]

Table IV. 7: Non-dimensional shear stresses $\bar{\tau}_{xz}(0, b/2, 0)$ for various power-law exponent of EG square and rectangular plates, $a/h = 10$.

b/a	Theory	Model	P						
			0.1	0.3	0.5	0.7	1.0	1.5	2
6	Present	PSDPT	0.46430	0.46350	0.46191	0.45954	0.45455	0.4425	0.42634
	Ref. [1] ^(*)	HSDPT	0.46330	0.46250	0.46091	0.45853	0.45357	0.44149	0.42525
	Zenkour [13]	TSDPT	0.47763	0.47686	0.47531	0.47299	0.46812	0.45639	0.44047
5	Present	PSDPT	0.45884	0.45805	0.45648	0.45414	0.44921	0.43735	0.42132
	Ref. [1] ^(*)	HSDPT	0.45785	0.45707	0.45549	0.45314	0.44824	0.43630	0.42025
	Zenkour [13]	TSDPT	0.47202	0.47125	0.46972	0.46743	0.46262	0.45102	0.43530
4	Present	PSDPT	0.44912	0.44835	0.44681	0.44452	0.43969	0.42809	0.41240
	Ref. [1] ^(*)	HSDPT	0.44816	0.44738	0.44584	0.44354	0.43875	0.42706	0.41135
	Zenkour [13]	TSDPT	0.46202	0.46127	0.45977	0.45753	0.45281	0.44147	0.42607
3	Present	PSDPT	0.42946	0.42872	0.42726	0.42506	0.42045	0.40935	0.39435
	Ref. [1] ^(*)	HSDPT	0.42854	0.42780	0.42633	0.42413	0.41954	0.40837	0.39334
	Zenkour [13]	TSDPT	0.44180	0.44108	0.43965	0.43751	0.43300	0.42214	0.40742
2	Present	PSDPT	0.38172	0.38107	0.37977	0.37782	0.37371	0.36385	0.35051
	Ref. [1] ^(*)	HSDPT	0.38025	0.37894	0.37699	0.37291	0.36298	0.34962	0.38025
	Zenkour [13]	TSDPT	0.39205	0.39078	0.38887	0.38486	0.37522	0.36213	0.39205
1	Present	PSDPT	0.23852	0.23811	0.23729	0.23607	0.23351	0.22734	0.21900
	Ref. [1] ^(*)	HSDPT	0.23760	0.23678	0.23556	0.23301	0.22680	0.21845	0.23760
	Zenkour [13]	TSDPT	0.24496	0.24417	0.24298	0.24047	0.23444	0.22626	0.24496

^(*) Results taken from reference of Mantari and Guedes Soares [1]

IV.2.2 Parametric study

The available graphical representations of the results of the current parabolic plate theory, which uses four unknowns, are plotted with the results of previous research by Mantari and Guedes Soares [1]. Figures IV.1 to IV.7 display the axial and transverse displacements $(\bar{u}, \bar{v}, \bar{w})$ and stresses $(\bar{\sigma}_{xx}, \bar{\tau}_{xy}, \bar{\tau}_{xz}, \bar{\tau}_{yz})$ distributions through the thickness of thick exponentially graded plates ($a/h = 4$) for the different values of the aspect ratio ($a/b = 1, 2, 4$) and the power-law exponent value ($p = 0.5$) computed by means of the present formulations as well as by the governing differential equations of the proposed PSDPT model with four unknown variables and with the HSDPT developed by Mantari and Guedes Soares [1] based on the displacement field having five unknowns. Examination of these figures indicates that the proposed model produces good results compared with each other.

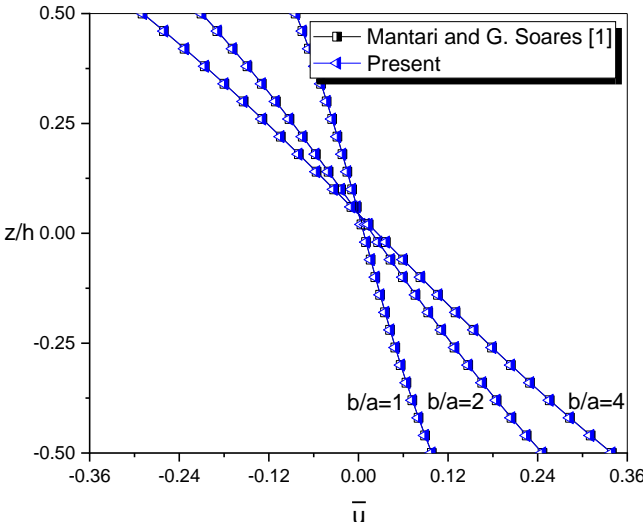


Figure IV.1: Distribution of non-dimensional axial displacement (\bar{u}) across the thickness of EG square and rectangular plates ($a/h = 4, p = 0.5$)

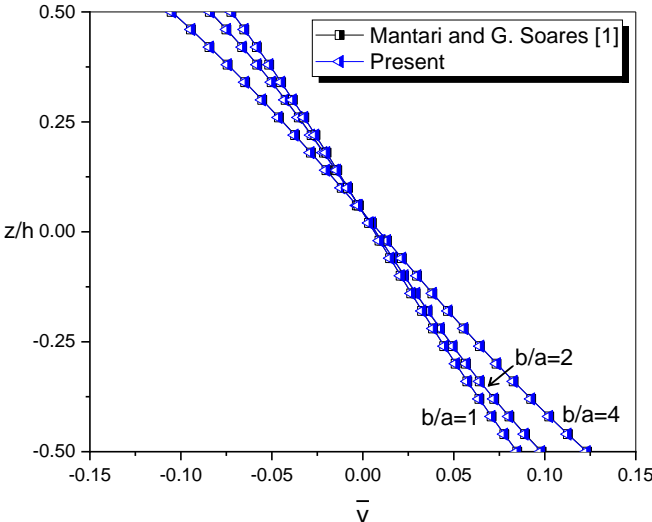


Figure IV.2: Distribution of non-dimensional axial displacement (\bar{v}) across the thickness of EG square and rectangular plates ($a/h = 4, p = 0.5$)

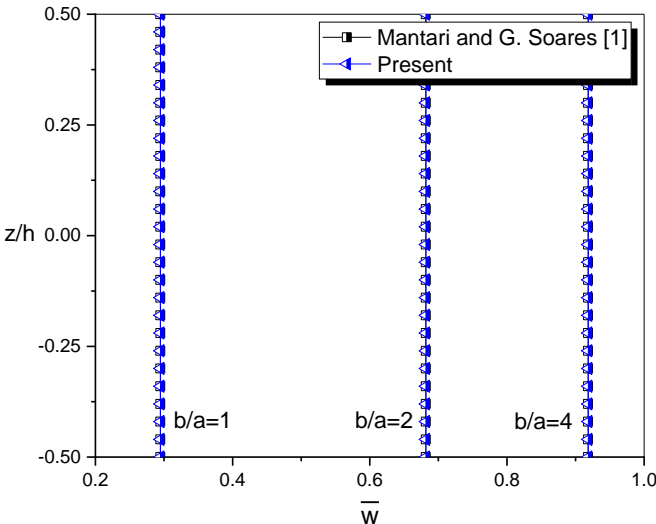


Figure IV.3: Distribution of non-dimensional transverse displacement (\bar{w}) across the thickness of EG square and rectangular plates ($a/h = 4, p = 0.5$)

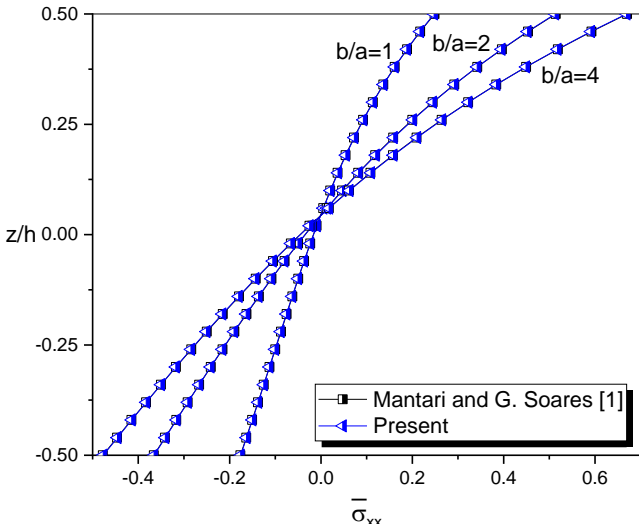


Figure IV.4: Distribution of non-dimensional axial stress ($\bar{\sigma}_{xx}$) across the thickness of EG square and rectangular plates ($a/h = 4, p = 0.5$)

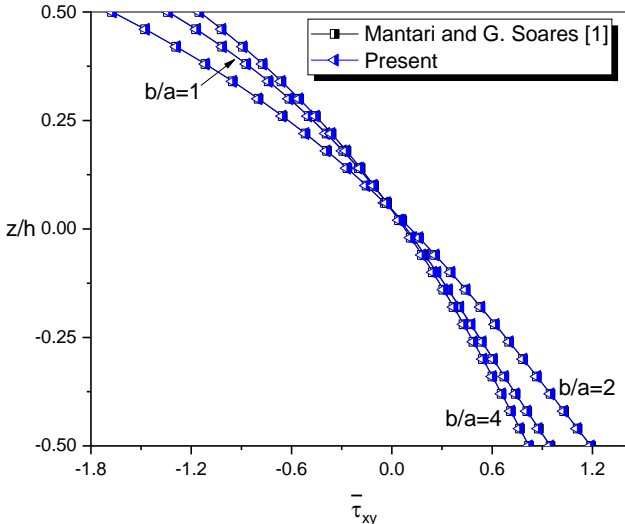


Figure IV.5: Distribution of non-dimensional in-plane shear stress ($\bar{\tau}_{xy}$) across the thickness of EG square and rectangular plates ($a/h = 4, p = 0.5$)

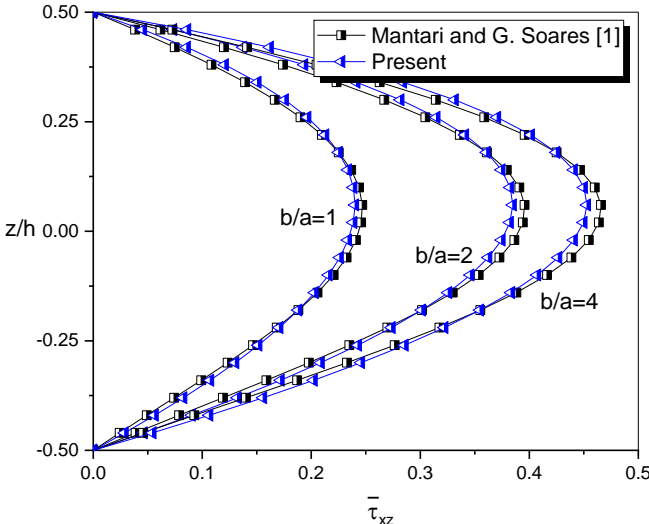


Figure IV.6: Distribution of non-dimensional transverse shear stress ($\bar{\tau}_{xz}$) , through the thickness of EG square and rectangular plates ($a/h = 4, p = 0.5$)

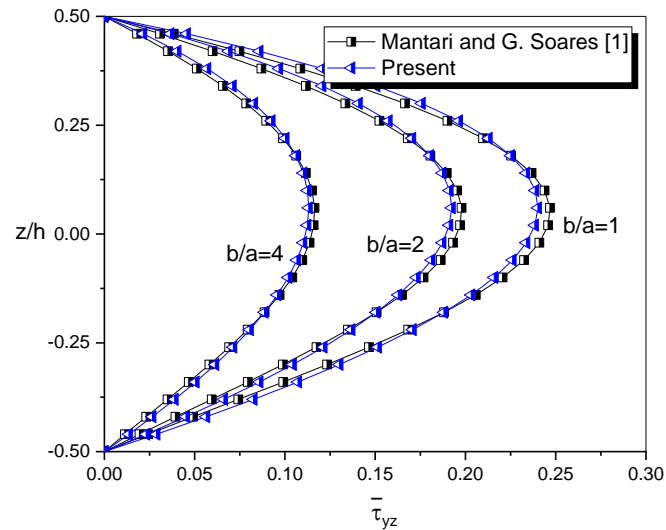


Figure IV.7: Distribution of non-dimensional transverse shear stress ($\bar{\tau}_{yz}$), through the thickness of EG square and rectangular plates ($a/h = 4$, $p = 0.5$)

IV.3. Conclusion

In this chapter, a new parabolic high-order shear deformation plate theory (PSDPT) with only four variables is presented for the analysis of the static behavior of thick plates without taking into account the thickness stretching effect. The governing equations are obtained from the virtual work principle. Analytical solutions are determined for simply supported square and rectangular plates. The number of variables is decreased in order to make the new theory simple and efficient to use. The numerical results show that these modified assumptions have a minimal influence on the accuracy of the results for the problems examined. Therefore, it can be deduced that the new (PSDPT) theory is not only accurate but also simple in predicting the bending response of functionally graded plates.

■ *General Conclusion*

Concluding remarks

In this study, a displacement field containing integrals with four variables is developed and applied for the static (mechanical) analysis of E-FGM plates. The present theory has the following features:

1. The present theory considers the effects of transverse shear deformations;
2. The present theory satisfies the traction free boundary conditions at top and bottom surfaces of the plates using the constitutive relation as well as does not require the problem dependent shear correction factor to determine strain energy due to shear deformation.

Based on the numerical examples solved and from the subsequent discussion, following conclusions are drawn:

1. The numerical results presented in this study represent that the present theory is more accurate than any other theory available in the literature while predicting the mechanical response of E-FGM plates. This is in fact due to consideration of effects of transverse shear deformation.
2. The present theory is in excellent agreement for predicting bending behavior of FG plates.

Future scope:

The present theory can be extended for many other problems in the field of FG structures. Some of them are listed below:

The present theory can be extended to study:

1. The static response of FG plates under thermo-mechanical, hygro-thermo-mechanical, and hygro-thermo-electro-mechanical loadings.
2. The buckling analysis of laminated composite and functionally graded sandwich shells.
3. Analyze the laminated composite shells for different boundary conditions.
4. Analyze the FGM plates considering the effects of porosity.

 *Bibliographic references*

Bibliographic references

- [1] Mantari, J.L., Guedes Soares, C. “Bending analysis of thick exponentially graded plates using a new trigonometric higher order shear deformation theory”, *Compos Struct*, 2012, 94, 1991–2000.
- [2] Hebbar, N. “Etude de l’effet de déformation de cisaillement sur la réponse statique et dynamique des structures composites épaisses”, Thèse de doctorat, Université de Djillali Liabes de Sidi Bel Abbes, 2018.
- [3] Belarouci, A. “Etude comparative du comportement des plaques épaisses P-FGM ET S-FGM”, Thèse de doctorat, Université de Djillali Liabes de Sidi Bel Abbes, 2021.
- [4] Sebakhi, F., Zemani, K. “Etude des vibrations libres des plaques épaisses en matériaux à gradient fonctionnel (FGM) reposant sur un support élastique de Winkler-Pasternak”, Mémoire de master structures aéronautique, Blida : institut d’aéronautique et des études spatiales, 2015.
- [5] Cheng, Z.Q., Batra, R.C. “Deflection relationships between the homogeneous Kirchhoff plate theory and different functionally graded plate theories”, *Arch Mech*, 2000, 52, 143–58.
- [6] Javaheri, R., Eslami, M.R. “Thermal buckling of functionally graded plates based on higher order theory”, *J Therm Stresses*, 2002, 25(7), 603–625.
- [7] Kashtalyan, M. “Three-dimensional elasticity solution for bending of functionally graded plates”, *Eur J Mech A/Solid*, 2004, 23, 853–64.
- [8] Carrera, E., Brischetto, S., Robaldo, A. “A variable kinematic model for the analysis of Functionally Graded Materials plates”, *AIAA J.*, 2008, 46, 194–203.
- [9] Ferreira, AJM, Batra, RC, Roque, CMC, Qian, LF, Martins, PALS. “Static analysis of functionally graded plates using third-order shear deformation theory”, *Compos Struct*, 2005, 69, 449–57.
- [10] Elishakoff, I. “Three-dimensional analysis of an all-round clamped plate made of functionally graded materials. *Acta Mech*, 2005, 180, 21–36.
- [11] Zenkour, A.M. “Generalized shear deformation theory for bending analysis of functionally graded plates”, *Appl Math Model*, 2006, 30, 67–84.
- [12] Chi S.H., Chung Y.L. “Mechanical behavior of functionally graded material plates under transverse load. Part I: analysis”, *Int J Solids Struct*, 2006, 43, 3657–3674.
- [13] Zenkour, A.M. “Benchmark trigonometric and 3-D elasticity solutions for an exponentially graded thick rectangular plate”, *Appl Math Model*, 2007, 77, 197–214.

- [14] Mantari J.L., Oktem A.S., Guedes Soares, C. “A new trigonometric shear deformation theory for isotropic, laminated composite and sandwich plates”, *Int J Solids Struct*, 2012, 49, 43–53.
- [15] Levy, M. “Memoire sur la théorie des plaques élastique planes”, *J Math Pures Appl* 1877, 30, 219–306.
- [16] Stein M. “Nonlinear theory for plates and shells including the effects of transverse shearing” *AIAA*, 1986, 24(9), 1537–1544.
- [17] Touratier M. “An efficient standard plate theory”, *Int J Eng Sci*, 1991, 29(8), 901–916.
- [18] Thom, V.D., Dinh, K.N., Nguyen, D.D., Duc, H.D., Tinh, Q.B. “Analysis of bi-directional functionally graded plates by FEM and a new third-order shear deformation plate theory”, *Thin-Walled Struct*, 2017, 119, 687–699.
- [19] Bennai, R., Fourn, H., Ait Atmane, H., Tounsi, A. and Bessaim, A., “Dynamic and wave propagation investigation of FGM plates with porosities using a four variable plate theory”, *Wind Struct*, 2019, 28(1), 049–62.
- [20] Zaitoun, M.W., Chikh, A., Tounsi, A. et al. “An efficient computational model for vibration behavior of a functionally graded sandwich plate in a hygrothermal environment with viscoelastic foundation effects”, *Eng Comput*, 2021,
- [21] Shailendra Kumar Bohidar, *Functionally Graded Materials: A Critical Review*, *International Journal of Scientific Footprints*, 2014, 2(4), 18 -29.
- [22] Yan Li, Zuying Feng, “A review on functionally graded materials and structures via additive manufacturing: from multi-Scale design to versatile functional properties”, *advanced Materials technologies*, 2020.
- [23] Isaac E., Demetris P., Cristina G. “Mechanics of functionally graded material structures”, *world scientific*, Singapore, 2016.
- [24] ITT, N., “Etude du comportement statique des structures en matériaux avancés FGMs en utilisant la théorie de déformation de cisaillement”, *mémoire de master*, Université Dr Moulay Tahar de Saida, 2017.
- [25] Hebbar, I., “Analyse par la méthode des éléments finis du comportement en rupture des matériaux FGM”, *thèse de doctorat*, Université de Djillali Liabes de Sidi Bel Abbes, 2022
- [26] Miyamoto, Y. et al. “FUNCTIONALLY GRADED MATERIALS Design, Processing and Applications”, *Springer Science+ Business Media*, 1999.

- [27] Benbakhti, A. “Modélisation du comportement thermomécanique des plaques FGM (Functionally Graded Materials)”, thèse de doctorat, Université Abdelhamid Ibn Badis Mostaganem, 2017.
- [28] Hui-Shen, S. “Functionally graded materials; Nonlinear analysis of plates and shells”, edition Taylor & Francis Group, New York, 2009.
- [29] Ghali, B., Guellil, H. “Solution analytique par la théorie de l'élasticité des poutres consoles en FGM soumises à charges d'ordres supérieure”, mémoire de master, Université Ibn khaldoun de Tiaret, 2021.
- [30] Younsi, A. “Proposition d'une théorie de déformation de cisaillement 2D et 3D pour l'étude du comportement mécanique des plaques”, thèse de doctorat, Université de Djillali Liabes de Sidi Bel Abbes, 2019.
- [31] Yousfi, M. “Etude de l'effet de porosités sur le comportement mécanique des structures FGM”, thèse de doctorat, Université de Djillali Liabes de Sidi Bel Abbes, 2020.
- [32] Popoola, P. et al. “Laser Engineering Net Shaping Method in the Area of Development of Functionally Graded Materials (FGMs) for Aero Engine Applications - A Review”, fiber laser, INTECH, 2016.
- [33] Mohammadi, M., Rajabi, M., Ghadiri, M. “Functionally graded materials (FGMs): A review of classifications, fabrication methods and their applications, Processing and Application of Ceramics”, 2021, 15(4), 319–343.
- [34] Addou, F.Y. “Analyse statique et dynamique des structures FGM : formulation théorique et application dans le domaine de génie civil”, thèse de doctorat, Université de Djillali Liabes de Sidi Bel Abbes, 2021
- [35] Mahmoud, D., Elbestawi, M.A. “Lattice Structures and Functionally Graded Materials Applications in Additive Manufacturing of Orthopedic Implants: A Review”, journal of manufacturing and materials processing, 2017, 1, 13.
- [36] Rasheedat, M. Mahamood, et al. “Functionally Graded Material: An Overview”, Proceedings of the World Congress on Engineering, Vol III, 2012
- [37] Said, A. “Etude et analyse des plaques FGM en Génie Civil”, thèse de doctorat, Université de Djillali Liabes de Sidi Bel Abbes, 2015.
- [38] Amanett, A. , Bouait, F. “Analyse et modélisation du comportement statique des poutres en matériaux à gradient de propriété sous l'effet de cisaillement transverse”, mémoire de master, Université Ibn khaldoun de Tiaret, 2012.

- [39] Chung, Y.L., Chi, S.H., “The residual stress of functionally graded materials”, *J. Chin. Inst. Civ. Hydraul. Eng.*, 2001, 13, 1–9.
- [40] MERZOUG, M. “Contribution à l’étude des structures composites sous chargement thermomécanique – comparaison entre les structures épaisses et mince”, thèse de doctorat, Université de Djillali Liabes de Sidi Bel Abbès, 2021.
- [41] Reddy, J.N. “theory and analysis of elastic plates and shells”, 2nd edition, Taylor & Francis Group, New York, 2007.
- [42] Reissner, E. “The effect of transverse shear deformation on the bending of elastic plates”, *ASME J. of App. Mech.*, 1945, 12, 69–77.
- [43] Mindlin, R.D. “Influence of rotatory inertia and shear on flexural motions of isotropic, elastic plates”, *J. of App. Mech.*, 1951, 18, 31–38.
- [44] Ambartsumian, S.A. “Principal equations and correlations in different modulus theory of elasticity of anisotropic bodies”, *Izvestija ANSSSR, MTT*, 3, 1969.
- [45] Reddy, J. N. “A simple high-order theory of laminated composite plate”, *J. App. Mec. (Trans. ASME)*, 1984, 51, 745–752.
- [46] Touratier, M. “An efficient standard plate theory”, *Int. Journal Eng. Sci*, 1991, 29(8), 901–916.
- [47] Karama, M., Afaq, K.S., Mistou, S. “Mechanical behaviour of laminated composite beam by new multi-layered laminated composite structures model with transverse shear stress continuity”, *Int J Solids Structures*, 2003, 40(6), 1525–1546.
- [48] Kirchhoff, G.R. “Über das gleichgewicht und die bewegung einer elastischen scheinbe”, *J. for Pure and App. Math.*, 1850, 40, 51–88.
- [49] K.P. Soldatos, “A transverse shear deformation theory for homogeneous monoclinic plates”, *Acta Mech*, 1992, 94, 195–200.
- [50] Aydogdu, M. “Vibration analysis of cross-ply laminated beams with general boundary conditions by Ritz method”, *International Journal of Mechanical Sciences*, 2005, 47, 1740–1755.
- [51] Zenkour, A. M. “Thermal bending of layered composite plates resting on elastic foundations using four-unknown shear and normal deformations theory”, *Composite Structures*, 2015, 122, 260–270.
- [52] Shimpi, R.P. “Refined plate theory and its variants”, *AIAA Journal*, 2002, 40 (1), 137–146.
- [53] Shimpi, R.P. and Patel, H.G. “A two variable refined plate theory for orthotropic plate analysis”, *Int. J. Solids Struct.*, 2006, 43, 6783–6799,

- [54] Zenkour, A.M, “A quasi-3D refined theory for functionally graded single-layered and sandwich plates with porosities”, *Composite Structures*, 2018, 201, 38–48.
- [55] Alibeigloo, A. “Exact solution for thermo-elastic response of functionally graded rectangular plates”, *Compos Struct*, 2010, 92(1), 113–121.
- [56] Vel, S.S., Batra, R.C. “Three-dimensional exact solution for the vibration of functionally graded rectangular plates”, *J. Sound Vib.*, 2004, 272, 703–730.
- [57] Uymaz, B. and Aydogdu, M. “Three-Dimensional Vibration Analyses of Functionally Graded Plates under Various Boundary Conditions”, *Journal of Reinforced Plastics and Composites*, 2007, 26(18), 1847–1863.
- [58] Di Sciuva, M. “Bending, vibration and buckling of simply supported thick multilayered orthotropic plates: An evaluation of a new displacement model” *J. Sound Vtbr.*, 1986, 105, 425–442.
- [59] Kablia, A. “Effet de la porosité sur le comportement mécanique des plaques en matériau à gradient de propriétés sous diverses conditions aux limites: analyse et modélisation”, thèse de doctorat, Université Ibn khaldoun de Tiaret, 2023.